September 27, 2012

APPROVAL SHEET

Title of Dissertation: **"Generation and Characterization of a Double Recombinant Monkeypox Virus for use in Animal Model Development and Therapeutic Evaluation"**

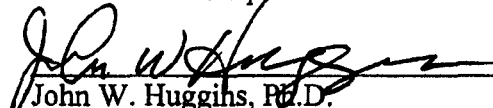Name of Candidate: **Kenny L. Lin**, Master of Science **in Emerging Infectious Diseases**
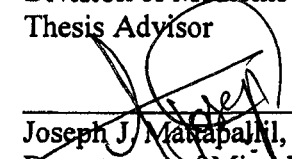
09/27/2012

THESIS AND ABSTRACT APPROVED:

DATE:

Dr. Gerald V. Quinnan, Jr., M.D.
Department of Preventative Medicine
Committee Chairperson
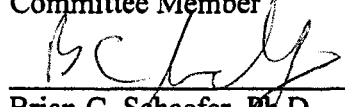
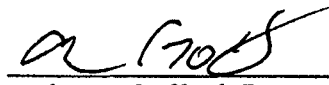John W. Huggins, Ph.D.
Division of Medicine (USAMRIID)
Thesis Advisor

Joseph J. Mattapallil, Ph.D.
Department of Microbiology and Immunology
Committee Member

Brian C. Schaefer, Ph.D.
Department of Microbiology and Immunology
Committee Member

Arthur J. Goff, Ph.D.
Virology Division (USAMRIID)
Committee Member

Copyright Statement

The author hereby certifies that the use of any copyrighted material in the thesis manuscript entitled:

"Generation and Characterization of a Double Recombinant Monkeypox Virus for use in Animal Model Development and Therapeutic Evaluation"

is appropriately acknowledged and, beyond brief excerpts, is with the permission of the copyright owner.

Kenny L. Lin
Emerging Infectious Disease Program
Uniformed Services University
09/27/2012

Abstract

Title of Thesis: Generation and Characterization of a Double Recombinant Monkeypox Virus for use in Animal Model Development and Therapeutic Evaluation

Kenny L. Lin, Master of Science, 2012

Thesis directed by: John W. Huggins, Ph.D.
Senior Scientist, Dept. of Clinical Research, Division of Medicine
United States Army Medical Research Institute of Infectious Diseases
(USAMRIID)
Secondary Faculty Appointment: Department of Emerging Infectious
Diseases

Monkeypox virus (MPXV) is an emerging/re-emerging zoonotic infection endemic to Central

Africa that produces a human disease similar to smallpox. Since the cessation of active

vaccination and the global eradication of smallpox, monkeypox has emerged as a potential

biological threat due to the vast number of unvaccinated individuals worldwide. Given the

adverse events associated with current vaccination strategies, and a lack of fully licensed

therapeutic options, there has been sustained interest in countermeasure development, testing,

evaluation, and implementation. The continued development of animal models to replicate

human disease has been crucial for therapeutic evaluation, and while no current model

recapitulates all the features of human disease, nonhuman primate models have come close.

Here, we describe the construction of a new double recombinant fluorescent monkeypox virus

(MPXV-GFP-tdTR), validate its use for therapeutic evaluation *in vitro,* and demonstrate its

pathogenicity in nonhuman primates. The data support the prospective use of this virus for future

animal model development and therapeutic evaluation studies.

Generation and Characterization of a Double Recombinant Monkeypox Virus for use in Animal Model Development and Therapeutic Evaluation

By

Kenny L. Lin

Thesis submitted to the Faculty of the
Emerging Infectious Diseases Program
Uniformed Services University of the Health Sciences
In partial fulfillment of the requirements for the degree of
Master of Science 2012

Dedication

To all my family and friends
who have given their support

Acknowledgements

To Dr. Sara Johnston and Dr. Arthur Goff, I thank you for all your time, energy, and guidance in helping me through this long journey. To my thesis committee: Dr. Gerald Quinnan, Dr. Joseph Mattapallil, Dr. Brian Schaefer, and Dr. John Huggins, I thank each of you for your patience, understanding, and support. To Dr. Lee Metcalf, thank you for always being available and supporting me throughout this entire process.

To Ms. Jacqueline Gearhart, thank you for all the hours upon hours of assistance with the flow cytometry experiments, I cannot begin to express my deepest appreciation for your help.

To all my friends, classmates, teammates, and past officemates, thank you for making me laugh and giving me the opportunity to enjoy the other aspects of life.

To my fellow scientists (past and present) at USAMRIID, thank you for your training, mentorship, expertise, reagents, and time. It has been a great experience learning from each of you. A special thank you to the Veterinary Medicine staff in particular for fulfilling all those countless blood requests.

To Lauren and Grace, thank you for all your support and patience. Both of you always find a way to make me smile and laugh even during the most trying times.

Finally, to my parents who have always had my best interests at heart and provide unlimited, unconditional, and unwavering love and support in whatever decisions I make – I cannot thank you enough.

Table of Contents

List of Figures

List of Tables

Introduction

Background

Orthopoxviruses

The Family *Poxviridae* consists of two Subfamilies: *Chordopoxvirinae* (vertebrate hosts) and *Entomopoxvirinae* (insect hosts). *Chordopoxvirinae* is separated into eight Genera: *Orthopoxvirus, Parapoxvirus, Avipoxvirus, Capripoxvirus, Leporipoxvirus, Suipoxvirus, Molluscipoxvirus,* and *Yatapoxvirus*. The genera *Orthopoxvirus* is responsible for the majority of human disease and mortality caused by the *Poxviridae* family of viruses. (19)

Orthopoxviruses are large, complex, double stranded DNA viruses which, unlike most other viruses, replicate solely within the cytoplasm of an infected cell. The genome can range in size from 130-300kb, and the virion has a brick like structure as viewed through electron microscopy (EM) imaging. The virion contains 4 main structures: a nucleosome core, lateral body, membrane, and envelope. There are two main infectious forms of the virus; a mature virion (MV) and an extracellular enveloped virion (EV). (19)

The virus replication cycle (Fig. 1) is complex and begins with the attachment of an infectious virion to a cellular receptor. MVs have been shown to bind cell surface glycosaminoglycans or laminin, while EV attachment receptors have yet to be identified (41). Upon fusion with the plasma membrane or macropinocytosis, transcription of early gene proteins (transcription factors for intermediate genes, DNA/RNA polymerases, growth factors, and host cellular modifiers) occurs immediately (2). Once the viral core is uncoated, DNA replication occurs, providing a genomic template for intermediate and late gene transcripts (41). As late
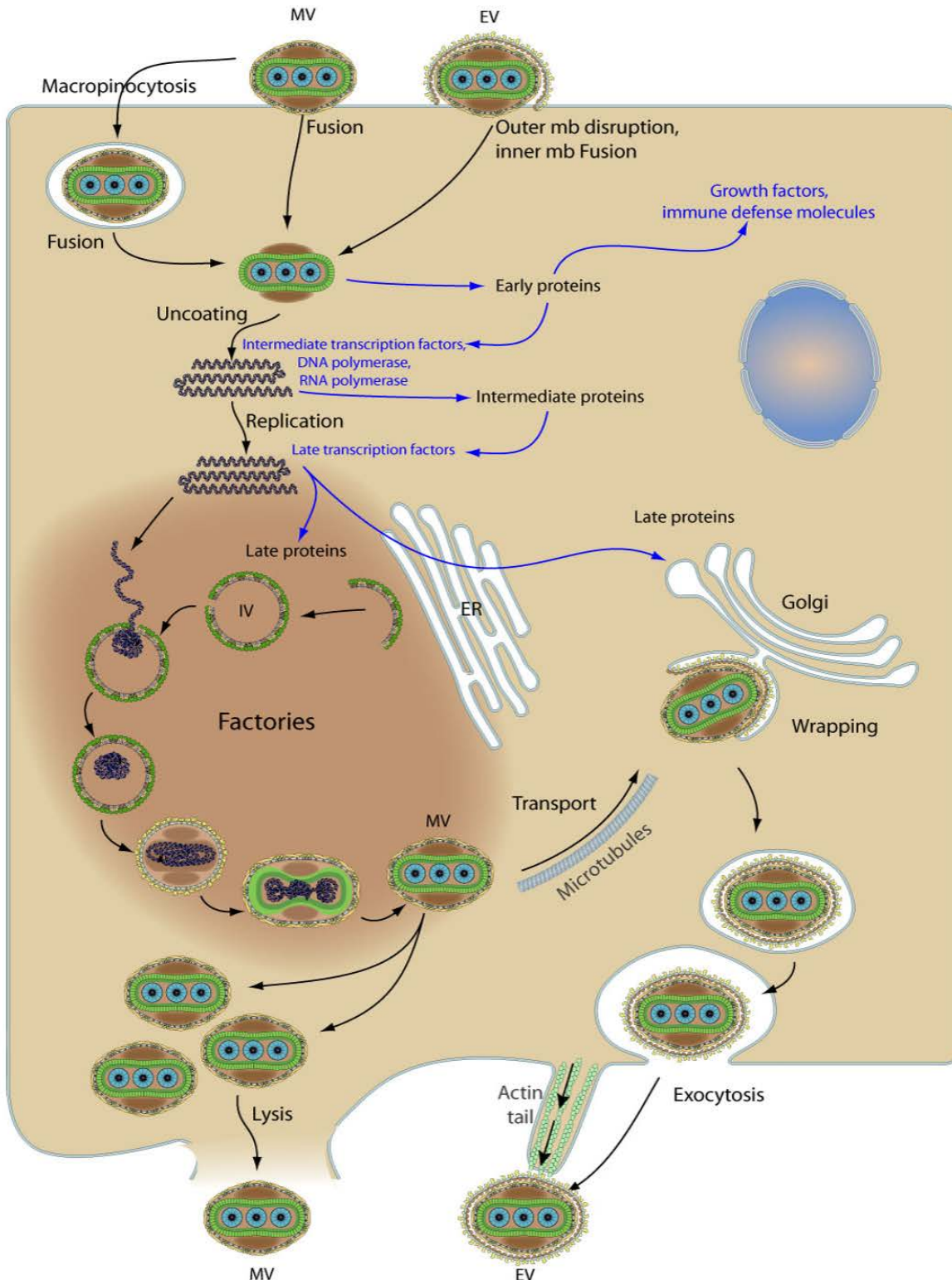
FIGURE 1. ORTHOPOXVIRUS REPLICATION CYCLE.
Visual depiction of orthopoxvirus entry, transcription, translation, virion assembly, and cellular exit processes within a permissive cell type. The process is complex, includes two infectious forms of the virus (MV and EV) and several distinct stages of gene expression. Figure obtained from http://education.expasy.org/images/Poxviridae_cycle.jpg (2)

proteins are generated (most of which are structural proteins and enzymes for virion assembly), electron dense inclusion bodies (viral factories) form near the endoplasmic reticulum (4). Virus assembly occurs within these inclusion bodies beginning with the formation of crescent-shaped lipoprotein structures that enclose viral core components into a spherical immature virion (4, 51). Morphogenesis occurs with the packaging of the DNA genome into the immature virion, followed by the cleavage of core proteins and the inclusion of structural polypeptides, ultimately leading to the formation of MVs which are released from the cell following lysis (4, 5, 52). Approximately 10% of MVs are shuttled by microtubules through the *trans*-golgi network or early endosomes where they acquire two additional membranes and become wrapped virions (WV) (41). WVs associate with the microtubule motor kinesin which carries these virions to the cell periphery via the microtubule network. It is here that the outermost membrane of the WV fuses with the plasma membrane, releasing EV onto the cell surface (61). Actin tail polymerization beneath the surface of EVs propel these virions toward adjacent cells, facilitating cell-to-cell spread (61). EVs can also be released from the cell surface, which contribute to systemic viral dissemination. The additional membrane surrounding EVs contain six distinct host proteins (different than MV membrane proteins), thought to protect the virions from normal host immune responses (4, 41).

Orthopoxviruses are genetically and antigenically similar. The central regions of the genome where structural genes involved in genome replication, morphogenesis, egress, binding, and entry are located are highly conserved (58). The terminal ends however, are much more variable; proteins expressed from this region are involved in immunomodulation and host range determination (40). These virulence factors are important for dictating cellular and host species tropisms, and ultimately disease progression (40). Terminal end divergence is a major factor in

understanding why certain orthopoxviruses cause no disease in humans (camelpox virus), whereas others can cause severe disease in humans (variola and monkeypox virus) (19). These differences also dictate how certain orthopoxviruses can infect a wide range of hosts (cowpox virus), whereas others are restricted to only one host (variola virus) (40).

Human disease and epidemiology

<u>Variola</u>

There are two distinct forms of smallpox: variola major, which causes the prototypical, highly virulent disease with a case fatality rate between 10-30%, and variola minor which causes a milder systemic disease with a case fatality rate less than 1%. Variola virus (VARV) is the only orthopoxvirus that causes disease in humans that is not zoonotic in nature. The most common transmission route is through the inhalation of aerosolized respiratory droplets, although documented contact with infectious material (fluids, scabs, and contaminated surfaces) also lead to disease development. (13)

Smallpox was a global pandemic that had devastating repercussions on dense unvaccinated populations. Due to the availability and relatively cheap production scheme for vaccine development, the World Health Organization (WHO) and the World Health Assembly launched a global eradication program in 1959. Widespread progress was not seen until 1967 when efforts were focused on increased surveillance and ring vaccination strategies to reduce the number of susceptible individuals. By late 1979, the WHO had declared smallpox eradicated. (36)

Smallpox disease progression in a natural setting was characterized by an asymptomatic incubation phase that lasted 10-14 days. This was followed by a febrile phase which lasted 3-4 days, during which time patients could reach a temperature near 103°F. The fever was typically

accompanied by headache, backache, vomiting, and prostration. A day or two following

incubation, a rash appeared on the extremities (face, mouth, palms and soles of the feet). Lesions

formed and progressed synchronously beginning with macular, advancing to papular, becoming

enlarged and vesicular by day 4 or 5, and ultimately pustular by day 7. Lesions began to scab and

encrust by day 14, eventually desquamating and leaving a pitted scar. The majority of cases

followed this disease progression; however, a small percentage (5%) of patients developed "flat

smallpox" which presented as slower developing lesions and associated with a higher case

fatality rate of 80%. Hemorrhagic smallpox occurred in less than 1% of all cases, where hallmark

symptoms included hemorrhage into the skin and mucosal membranes, a lack of lesion formation

and near uniform fatality within 1 week. (13, 19, 36)

Monkeypox

       Monkeypox virus (MPXV) is a zoonotic orthopoxvirus that produces a human disease

very similar to smallpox. First identified in 1958 in captive cynomolgus nonhuman primates

(10), MPXV contains 96.3% genomic homology with variola; however, they do not share an

orthopoxvirus genus ancestor and have genetic differences in the terminal ends of the genome

that are important for virulence and host range (14). MPXV is considered an emerging or re-

emerging infectious disease that naturally infects a number of wild animal (mostly rodent)

species, from which it can then be transmitted to humans. Due to the presence of reservoir hosts,

MPXV was able to survive beyond the global smallpox eradication campaign (10).

       The first human case was detected in 1970 in the Democratic Republic of Congo (DRC).

Clinical disease progression is nearly identical to normal human smallpox, which caused a

possible underreporting of active cases prior to the eradication of smallpox. Following exposure

to the virus, there is an incubation period that lasts 10 to 14 days. A typical prodrome period

(fever, malaise, headache, and backache) occurs 1 to 3 days prior to rash onset. Roughly 90% of human cases present with severe lymphadenopathy (unilateral or bilateral in several lymph node regions) 1 to 2 days post fever onset, a hallmark and key characteristic for distinguishing monkeypox from smallpox. Rash presentation is clinically indistinguishable from classical smallpox and occurs in a centrifugal pattern. Lesions progress through the characteristic macular, papular, vesicular, and pustule phases, culminating in scabs which desquamate leaving dyspigmented scars. The disease course generally lasts 4-5 weeks and severity is correlated with age, previous vaccination, nutritional, and immunological status. Monkeypox has a case fatality rate of approximately 10%, with most deaths occurring in unvaccinated children. (10, 14)

Ecological studies conducted in the DRC identified direct contact with reservoir species (rope squirrels, pouched rats, and dormice) account for the majority of primary transmission cases (21). Secondary (human-human) transmission occurred through either inhalation of aerosolized virus or direct contact with infected individuals or contaminated material. Most secondary cases occurred in households of infected individuals, often involving unvaccinated children. Serological surveillance studies conducted from 1970 – 2003 illustrate the distribution of human cases across the densely forested regions of Western and Central Africa (Fig. 2). Several hundred cases were confirmed during this time frame; including a large outbreak that occurred in 1996-97 where there were 511 cases, a significant number of which were attributed to secondary transmission. (10, 14, 21)

In 2003, monkeypox was introduced into the United States when infected rodents from Ghana (West African country) were imported into Texas (Fig. 3). Gambian rats were transported to Iowa, then Chicago where they were co-housed with prairie dogs. Infected prairie dogs were sold and distributed across multiple states including Wisconsin, Illinois, Indiana, Missouri,
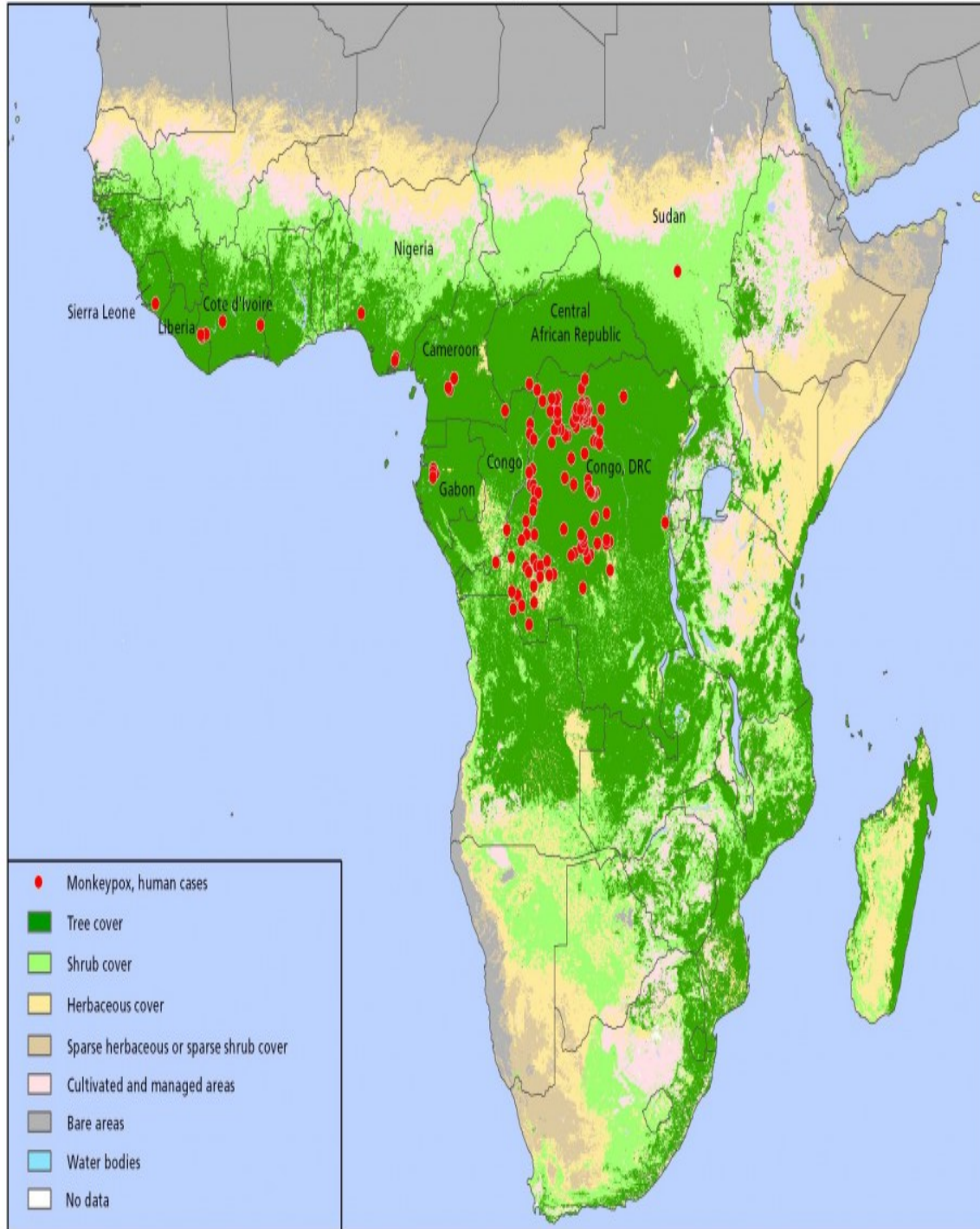
FIGURE 2. HUMAN MONKEYPOX DISTRIBUTION IN AFRICA.
Confirmed cases of human monkeypox disease distribution throughout Africa from 1970-2003 are shown in red. The distribution demonstrates the geographical separation of the two infectious clades (Western vs. Central) where the majority of cases are located in the Democratic Republic of Congo (DRC). Data originally obtained from Levine, 2007 (38) updated by Wertheim, 2012 (64) in 2011.

Kansas, and Ohio and were the primary infection source for patients who developed disease. In total, 71 cases were reported; of those, 37 were laboratory confirmed, and 10 were deemed probable cases. None of the cases were associated with secondary transmission, patients appeared to have a milder form of the disease (less severe rash), and none were fatal. (10, 14) Upon further evaluation, it was determined that MPXV exists as two distinct clades: Western Africa/USA and Congo Basin. Genetic changes in complement control protein C3L, which is truncated in the western clade virus, contribute to differences in virulence and pathogenesis (29, 39). C3L is a secreted complement control protein that prevents the normal recruitment and activation of complement, an important mediator in the recruitment of immune cells required for controlling infections (29). The deletion of C3L from the Congo Basin clade virus reduced morbidity and mortality in prairie dogs infected intranasally (29).

Since 1986, passive surveillance in the DRC has been the only source of information about monkeypox in this region. An insufficient health care system coupled with poor infrastructure made passive reporting extremely inaccurate, and the true health burden and geographic range of monkeypox was uncertain. In November of 2005, active surveillance was initiated in the DRC. This study surveyed the same health zones in the DRC that were assessed during the WHO active disease surveillance program conducted from 1981-1986. Between November 2005 and November 2007, 760 cases of active monkeypox were confirmed by MPXV-specific PCR. This number represented a significant increase in prevalence in this region 30 years following the cessation of smallpox vaccination. Decreasing herd immunity, poor health care, malnutrition, and secondary infections (particularly HIV) were a few of the factors that made this population extremely susceptible to MPXV infection. As in the 1980s, most of the cases occurred in unvaccinated individuals under the age of 30, and most occurred in health
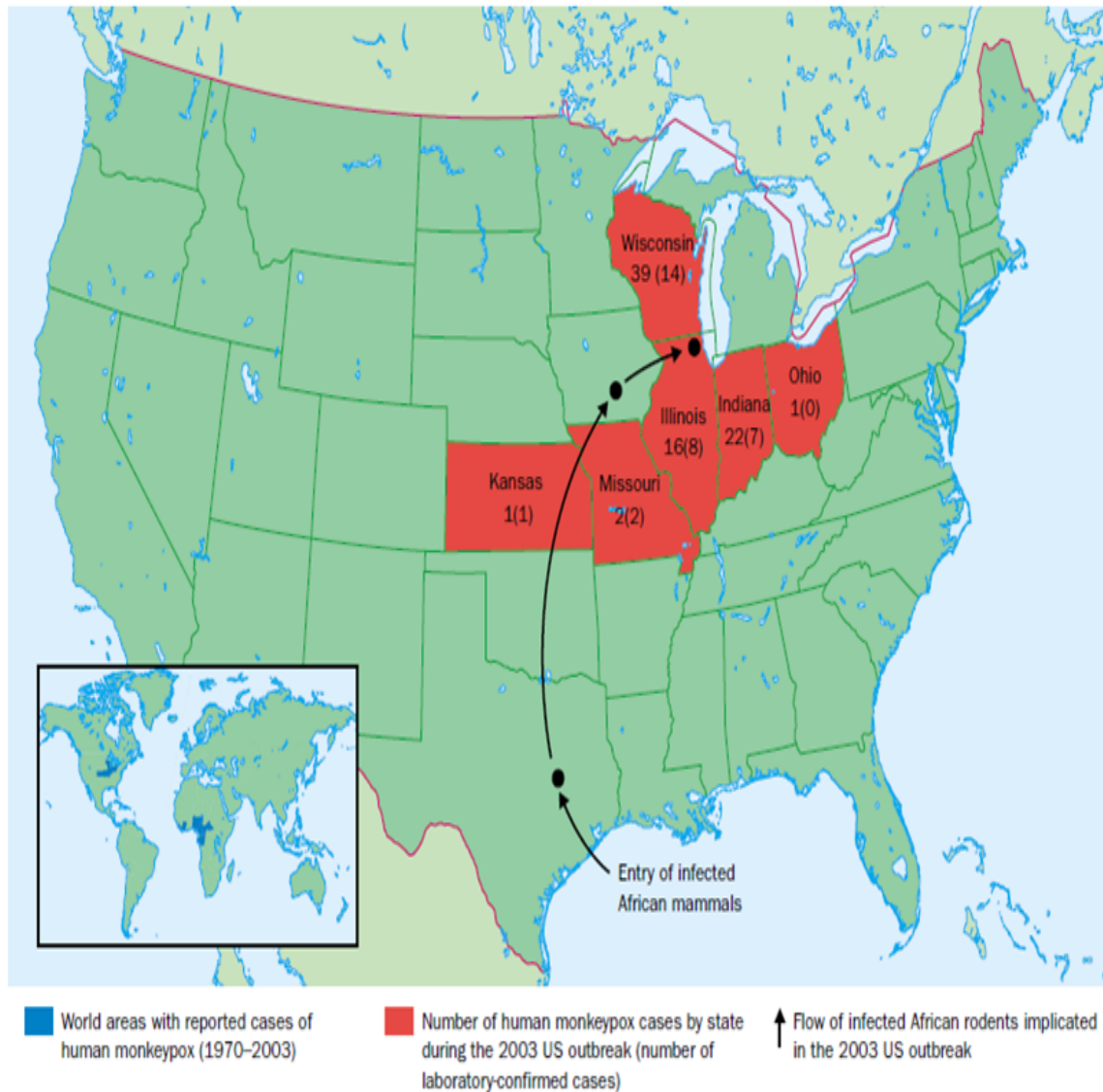
FIGURE 3. HUMAN MONKEYPOX DISTRIBUTION IN THE UNITED STATES.
Human monkeypox cases occurred in the U.S.A. in 2003 due to the importation of infected Gambian rodents that were co-housed with prairie dogs. Of the 71 reported cases, 37 were laboratory confirmed, 10 were probable cases, and none were fatal. Figure obtained from Di Guillo, 2004 (14).

zones located in forested areas where humans are brought into close contact with animal reservoirs. L'Hôpital Général Référence de Kole, one of the two sites of the original monkeypox investigation has continued to report roughly 100 cases per year for the past 30 years. (21, 31, 51)

Monkeypox virus is a threat to military forces operating in endemic regions and to the US. Its potential for epidemic human-to-human spread in large urban populations is unknown, and it remains a viable bioterrorism threat. New disease prevention strategies are being development to combat the accidental or deliberate release of smallpox and monkeypox.

Disease Prevention

Nonhuman primate animal models

One of the main challenges in any vaccine or therapeutic development program is the creation of animal models that accurately represent human disease when efficacy studies cannot be conducted in humans. Three hallmarks of a successful animal model include similar disease course as seen in humans, a natural route of infection, with a natural infectious dose. To fulfill the animal efficacy rule as set forth by the FDA, several different animal models have been developed that replicate orthopoxvirus disease in humans to varying degrees.

Current animal models in orthopoxvirus research span across multiple virus and animal species. A partial list of available models for variola and monkeypox is depicted in Table 1. The only variola animal model exists in nonhuman primates (*Cynomolgus Macaques)*, which were infected with a very high infectious dose intravenously (IV). Though the infection route/dose was highly unnatural, the animals developed disease similar to what was seen in human cases of smallpox. The mortality rate was approximately 33%, which correlated with human disease. (30)

Virus/Natural Host Species	Animal Model	Infection Route	Dose (pfu)	Primary Lesions/Disease
Variola/Human	Cynomolgus Macaque	IV	10^9	Hemorrhages, hemorrhagic effusions, early enanthema/exanthema
		IV	10^8	Enanthema/exanthema
		Aerosol	$10^{8.5}$	Mild pulmonary disease and exanthema
Monkeypox/ Rodent (squirrel)	Rhesus Macaque	IV	2×10^7	Vesiculopustular rash, lymphadenopathy
	Cynomolgus Macaque	IV	5×10^7	Vesiculopustular rash, lymphadenopathy, splenomegaly
		Aerosol	10,000 – 141,00	Fibrinonecrotic bronchopneumonia, necrotizing dermatitis, lymphoid necrosis
		IT	10^7	Fibrinonecrotic bronchopneumonia, necrotizing dermatitis, lymphoid necrosis
		IT	10^6	Mild necrotizing bronchopneumonia
Monkeypox/ Rodent (squirrel)	Black-tailed Prairie Dog	IP	12,600	Splenic necrosis, hepatic necrosis
		ID	25,200	Pulmonary edema, hemorrhage, necrosis
Monkeypox/ Rodent (squirrel)	13-lined Ground Squirrel	IP	12,600	Centrilobular hepatic necrosis, interstitial pneumonia
		IN	25,200	Diffuse hepatic necrosis, interstitial pneumonia
		SC	100	Multifocal splenic and hepatic necrosis, edema, hemorrhage

TABLE 1. ANIMAL MODELS OF ORTHOPOXVIRUS INFECTION.
A partial list depicting animal models of VARV and MPXV infection detailing primary lesion and disease development. Information obtained from Chapman, 2010 (7).

Since the eradication of smallpox, work with VARV was restricted to two locations, the CDC and the Vector laboratory in New Siberia; therefore, MPXV emerged as a surrogate model for smallpox disease (35). Challenges associated with working with MPXV include the use of Bio Safety Level 3+ (BSL-3+) facilities in conjunction with obtaining proper vaccinations, a Department of Justice (DOJ) registration number, and acceptance into an approved biosurety program. Concerns over MPXV's potential use for bioterrorism have earned it the classification as a Category C select agent according to the CDC select agent program (44), and as such, any laboratory work is highly regulated. There are currently several monkeypox specific animal models (Table 1) including infections of immunodeficient mouse strains, ground squirrels, prairie dogs, and nonhuman primates (NHP). Thus far, the NHP models have been the most representative of human disease and many studies have been conducted to characterize disease progression in regards to therapeutic evaluation (7).

The intravenous (IV) infection route of MPXV used with cynomolgus macaques as described by Huggins et al. (30) has been the primary NHP model for therapeutic evaluations due in part to the consistently high mortality rate (greater than 95%). Unfortunately, the model utilizes an extremely high infectious dose ($5x10^7$ plaque forming units - pfu) and an unnatural route of infection that bypasses primary viremia. As a result, the animals have an accelerated incubation period, but lesion development and progression is otherwise identical to that seen in human cases. The animals develop marked lymphadenopathy, splenomegaly and pulmonary edema (7). In some instances, animals develop and succumb within days to hemorrhagic monkeypox, which clinically resembles hemorrhagic human smallpox. (30, 32)

Upon confirmation that NHP infections could accurately represent human monkeypox disease, infection models focusing on respiratory challenge were developed to simulate a more

natural route of infection. Two such techniques involved the exposure of NHPs to MPXV with an automated bioaerosol exposure system with a three-jet collision nebulizer (aerosol) (43), and the deposition of inoculum directly into the left tertiary bronchus (IB) (33). In the aerosol model, animals were challenged with varying viral doses and succumbed to severe bronchopneumonia without systemic lesion development. Lesions were detected on the lungs at necropsy, and virus detection (IHC, ultrastructural, plaque assay) in the spleen, thymus, liver, and kidney demonstrated widespread distribution and viral replication. The IB infection route involved 3 mL of liquid inoculum ($5x10^5$ and $5x10^6$ pfu) deposited directly into the bronchial airway. The animals developed classical lesion distribution and high blood viral titers; however, uniform lethality was not observed. While both models more closely mimicked a natural infection route, each had its drawbacks which included expense, high and/or variable infection dose (aerosol), unnatural disease course, and non-uniform lethality.

To better address the issues of developing a more representative respiratory model of monkeypox infection, our group characterized a novel intratracheal (IT) exposure route as described by Goff et al. (24). To determine an appropriate infectious dose, three separate animal studies (n= 3 NHPs per study) using three different doses of virus ($3.42x10^6$, $8.37x10^6$, and $3.53x10^7$ pfu) were conducted. Animals were infected with 100 uL of virus inoculum just above the bifurcation of the trachea using a liquid MicroSprayer attached to a bronchoscope. This method ensured an even distribution of the virus within the lungs in a more manageable volume as compared to the IB model. The animals were monitored twice a day and evaluated for lesion development, viral blood titers, changes in blood chemistries, respiratory involvement, lymphadenopathy, and overall disease severity. (24)

All three infection doses resulted in classical monkeypox disease with blood viral titers greater than 10^6 by day 8 and 10 post-infection (24). The mortality rates for the respective infection doses were 33% (3.42×10^6 dose), and 66% (both 8.37×10^6 and 3.53×10^7 doses). Total lesion counts ranged from 100 – 500 and reached peak numbers by day 10 post-infection. Animals with severe disease had highly elevated blood urea nitrogen (BUN) levels and either succumbed or were humanely euthanized between day 10 and 16 post-infection. At the peak of disease, D8 and D10 post-infection, all animals demonstrated a spike in white blood cell (WBC) count and a reduction in red blood cell (RBC) count. There was an overall platelet increase (greater than 200%) in all animals that survived to the end of the study. (24)

Necropsy findings in animals that succumbed or were moribund included fibrononecrotic bronchopneumonia with edematous lungs that failed to collapse (24). Necrotic lesions were found along the trachea and on the outer surfaces of the lungs. Ulcerative lesions were seen on the oral mucosa, esophagus, stomach, and urinary bladder. Animals that survived infection had areas of necrosis in the lung, tracheal congestion along with enlarged peripheral lymph nodes, and desquamated skin lesions. (24)

Based on the disease manifestations and mortality rate, the 8.37×10^6 pfu dose was determined to be the optimal infection dose for this model (24). While this was still considered an "unnatural" dose, it was a log lower than the dose required in the IV model. While this model did not yield a uniformly fatal disease, it satisfied other aspects of a good animal model in that it utilized a lower infection volume and was more representative of how aerosol droplets are passed between individuals during orthopoxvirus transmission. To further characterize this model, follow up experiments tracking virus dissemination following lung infection would improve our

understanding of how monkeypox pathogenesis occurs. This model also represents another platform for therapeutic evaluation. (24)

Prevention and therapy

Vaccines

The eradication of smallpox and the cessation of vaccination programs in the early 1980s has resulted in a largely susceptible human population. While the natural reoccurrence of smallpox is unlikely, fears regarding the intentional release of weaponized variola or monkeypox, and ongoing monkeypox outbreaks in Africa have prompted investigations into the development of new vaccine and therapeutic strategies. The ultimate goal is the continued creation of products that are cross-reactive and cross-protective against multiple orthopoxviruses.

During the eradication campaign, live vaccinia virus (most notably, Dryvax® in the USA) was administered percutaneously on the arm by the use of a bifurcated needle. A positive take to the vaccine was characterized by the formation of a localized skin reaction with vesicle, pustule, and finally scab formation which detached in 2 to 3 weeks. The most common side effects included low grade fever, headache, general malaise, and lymphadenopathy. The entire vaccination process took up to 4 to 5 weeks, though protection was seen much earlier and lasted several years. Immunocompetent individuals generated neutralizing antibodies that were cross-protective against both smallpox and monkeypox. (42)

As with any live vaccine there were adverse events, especially when administered to individuals who were immunocompromised or had severe skin conditions such as eczema or psoriasis (45). There was a risk of developing secondary complications such as eczema vaccinatum, generalized or progressive vaccinia, and myocarditis (45). Eczema vaccinatum occurred in individuals with eczema who were vaccinated or came into contact with vaccinated

15

individuals and presented as a vesicular or pustular rash with some systemic symptoms (67).

Progressive vaccinia occurred in immunocompromised individuals and was characterized as

necrotic lesions at the site of vaccination that failed to heal and the appearance of secondary

lesions on other areas of the body (67). Both complications were very serious and sometimes

fatal. Accidental ocular infections and generalized vaccinia, which was characterized by the

appearance of pustular lesions on secondary sites, were not associated with any immune

deficiencies and responded well to vaccinia immune globulin (VIG) therapy (67).

As stocks of vaccine dwindled, new vaccine candidates have been developed and

categorized into "generations." First generation vaccines are strains used during the eradication

campaign. Second generation vaccines (ACAM2000, Elstree-BN, and Cell-cultured smallpox

vaccine) are live vaccinia virus (VACV) strains grown and plaque picked in cell culture to

ensure a more uniform virus population as compared to the variants found in Dryvax. While

these vaccines elicit quantifiable levels of protection (neutralizing antibodies and T-cell immune

responses) similar to individuals vaccinated with Dryvax, they also have the potential to induce

the same secondary complications (27). Third generation vaccines (LC16m8, MVA, NYVAC)

use attenuated viruses to produce robust immune responses (42). MVA has been demonstrated to

provide protection against MPXV challenge in NHPs (57) and elicit a high neutralizing antibody

titer in phase II human trials (60, 65). Fourth generation vaccines are subunit vaccines (DNA or

protein based) that are orthopoxvirus-specific and designed to be safer with less adverse events

(45). Some of these next generation vaccine candidates have been shown to provide protection

against MPXV infections in NHPs (25, 28).

Therapeutics

There is currently no fully licensed therapeutic available for the treatment of

orthopoxvirus infections. Given the complications associated with current vaccines and the time

for a protective immune response to be generated, interest in the development of post-exposure therapeutics for orthopoxvirus infections has continued to increase.

Due to the complex replication cycle of orthopoxviruses, there are many potential targets for therapeutic disruption. One example is the use of vaccinia immune globulin (VIG), which is isolated from the plasma of individuals who have received the VACV vaccine. VIG has typically only been used for the treatment of patients who experience vaccine related adverse events. In theory, the neutralizing antibodies that comprise VIG would provide passive protection against cellular infection; however, the effectiveness of VIG as a primary treatment strategy has not been conclusively demonstrated. (13, 46)

There are three synthesized compounds (Cidofovir, CMX001, and ST-246) that have gained investigational new drug (IND) status for use against orthopoxvirus infections. Cidofovir and ST-246 have been shown to be protective against variola and monkeypox challenge in lethal NHP models (3, 30, 35, 36, 57). Safety testing for human use and further development are ongoing.

Cidofovir (Gilead Sciences) targets the virus DNA polymerase and prevents severe disease in NHP when given 48 hr post-infection (49). In its current formulation, the drug must be administered IV and may cause some nephrotoxicity (seen in one case following three doses). CMX001 (Chimerix) is a pro-drug of cidofovir that contains an additional lipid conjugate and provides a bioavailable platform for drug delivery. This newly designed pro-drug has the same mechanism of action, while the lipid conjugate increases the targeting and uptake of the drug in specific organs important for viral replication. It has been shown to be protective in multiple orthopoxvirus animal models (ectromelia/mice, rabbitpox/rabbits, monkeypox/NHPs), is being

developed for other DNA viruses (BK virus in transplant patients) and is now in clinical development for prophylactic use. (49)

ST-246 (Siga Technologies) targets the formation of extracellular enveloped virions (EV) by blocking the wrapping of mature virions (MV) during viral morphogenesis (36). Inhibiting this process reduces infectious virus production and release, thereby decreasing overall systemic dissemination. ST-246 is orally bioavailable and been shown to be protective post-exposure and after onset of lesions in animal models of orthopoxvirus infections. These studies include the treatment of NHP infected with either VARV (24 hours post-infection) or MPXV (3 days post-infection) (36). Blood viral titers remained low and were cleared within 6 days; and animals did not develop any lesions. ST-246 is being reviewed in "fast-track" status for FDA approval due to its antiviral effectiveness and low toxicity profile. (36)

VIG, cidofovir, CMX001, and ST-246 all directly target the virus by interfering with distinct stages of the virus life cycle (binding and entry for VIG, replication for cidofovir and CMX001, and morphogenesis for ST-246). Although targeting the virus directly is beneficial as it reduces pathogenesis while minimizing potential side effects, the development of drug resistant virus variants is a possibility as evidenced through the *in vitro* use of cidofovir and ST-246 (1, 66). An alternative strategy is to indirectly target the virus by enhancing the immunological response to the virus. Recently, it was shown that Interferon-β could reduce virus production, release, and spread *in vitro* when administered either prior to infection or up to 12 hr post-infection (34).

Interferon-βeta and MxA

Interferon (IFN) is a secreted cytokine that has antiviral properties. There are three main types: I, II, III. IFN-β is a type I interferon which is known to produce a direct response to viral

infections. The IFN-β signaling cascade can be induced either through the recognition of viral

specific proteins by host cell receptors, or through the binding of IFN by IFN receptors, which

are found almost ubiquitously. Once activated, a large subset of inducible genes are transcribed,

promoting the cell to enter an "antiviral" state. The antiviral response includes cell cycle arrest,

apoptosis, increased MHC class I/II expression and antigen presentation. Additionally, IFN-β

pre-treatment can enhance the cell's ability to produce more IFN-β, establishing a positive

feedback loop. IFN-β modulates the immune response by promoting the maturation of dendritic

cells, increasing natural killer cell activity, and promoting the division of memory CD8+ T-cells.

(50)

Orthopoxviruses, namely vaccinia, have been shown to produce at least 13 different

proteins (most are produced early in infection) that interfere with normal IFN activity (48). The

disruptions include blocking enzymatic processes within the cell to prevent downstream

transcriptional events and the secretion of decoy IFN receptors to prevent the induction of the

exogenous signaling cascade (48). The redundancy seen during the viral replication process

illustrates the importance of IFN production for controlling viral infections. The importance of

IFN-β was demonstrated in studies where recombinant vaccinia viruses that produced IFN-β

greatly attenuated the amount of virus replication seen within a murine cell line (11). The

potential *in vivo* use of IFN-β was demonstrated when rhesus monkeys (infected intradermally

with VACV) failed to develop lesions following intravenous IFN treatment (62).

Myxovirus resistance protein 1 (MxA) is a member of the dynamin superfamily of

GTPases that is highly regulated by IFN. MxA is found in the cytoplasm, is involved with

intracellular membrane trafficking, and forms ring-like oligomeric structures (26). It has been

shown to have antiviral activity by inhibiting the replication of influenza, measles, and specific

bunyaviruses (56). The effects of IFN- β on MxA induction as a potential antiviral strategy have only recently been evaluated for MPXV infections (34).

Fluorescent Viruses

Green fluorescent protein (GFP) is isolated from the *Aequorea* jellyfish. Enhanced GFP (eGFP) is a derivative generated by specific point mutations made to the original protein that alter its excitation peak and increase its stability (59). eGFP has an excitation peak of 488nm and emission peak between 507-509nm, making it a popular fluorophore in cellular biology due to its similarities to fluorescein (FITC), the most widely used small molecule fluorophore. One of the first uses of eGFP was the fusion to specific cellular promoters to examine gene expression without the use of any enzymatic substrates. Cells actively producing the protein emitted green light under the right excitation sources and could be detected using multiple techniques (flow cytometry, fluorescence microscopy, microplate reader, and confocal microscopy). eGFP has also been used to create fusion proteins that allow for the identification and visualization of specific proteins and organelles within a cell. (59)

Tandem dimer tomato red (tdTR) is a derivative of a monomeric red fluorescent protein, which is isolated from the *Discosoma* species of coral. To increase stability and fluorescence intensity, "gfp-type C- and N-terminal ends" are inserted and two copies of the gene are fused together to prevent aggregation (55). The excitation and emission peaks for tdTR are 554nm and 581nm respectively, which allows for concurrent use with eGFP.

Studies have shown that recombinant VACV with eGFP under the control of viral promoters can be used to demonstrate infection within specific cell populations *in vitro* (15, 54). In most studies, eGFP was under the control of a synthetic vaccinia virus early/late promoter which produced eGFP early during infection (6). In other studies, recombinant MVA was

constructed to express eGFP, which allowed for the rapid detection of neutralizing antibody responses in vaccinated individuals and demonstrated the extended use of fluorescent proteins in vaccine and therapeutic evaluations (9).

The generation of double recombinant viruses expressing different fluorescent proteins under different viral promoters is a powerful technique used to understand viral pathways and for the evaluation of therapeutics. Recent work using such recombinant vaccinia viruses demonstrated retention of normal growth kinetics and provided the platform for the discovery of a novel anti-orthopoxvirus compound (16, 17).

Fluorescent protein-expressing viruses have also been used in several different animal model systems to evaluate disease pathogenesis and immune response, and to evaluate novel therapeutics. For example, the use of eGFP expressing measles virus allowed researchers to track virus replication and dissemination within specific immune cell populations and tissues throughout the disease course in NHPs (12). Recombinant eGFP expressing CPXV and MPXV have also been characterized in animal models, showing only slight attenuation and allowing for visual representation of viral dissemination (22, 23).

Hypothesis

Until recently eGFP was the only fluorescent gene inserted into MPXV-Zaire 79 (22). While this recombinant virus could be used to demonstrate virus presence, its use for evaluating changes in productive vs. nonproductive infections during animal model development and therapeutic evaluation was limited. The original intended use for the generation of a double recombinant fluorescent MPXV was to test the hypothesis that monocyte derived cell types were preferentially targeted during monkeypox infections, and that subsequent changes in activation/maturation of the infected cells correlated with changes in the pro-inflammatory

21

cytokine profile, which would influence disease progression. The aims addressed in this thesis were to: i) demonstrate the proper generation and characterization of MPXV-GFP-tdTR, which contained two fluorescent genes under the control of different viral promoters and retained virulence; ii) validate the use of the virus in study of therapeutic drug effects; and iii) demonstrate disease in a nonhuman primate model of infection by the double recombinant virus. The generation of this recombinant virus was done with approval from the Institutional Biosafety Committee (IBC) within the United States Army Medical Research Institute of Infectious Disease (USAMRIID), and all experiments were conducted in highly regulated BSL-3+ containment laboratories.

Materials and Methods

Double Recombinant MPXV-GFP-tdTR

The expression plasmid pcDNA-DEST40 and its description map were provided by Drs. Mohamed Mohamed and Grant McFadden (University of Florida). The plasmid (Fig 4A) contains both the eGFP and tdTR fluorescent inserts. eGFP expression is under the control of a viral synthetic E/L promoter (early gene) while tdTR is under the vaccinia virus promoter 11 (late gene). Both fluorescent genes were targeted for insertion into the intergenic region between RPO22 and UNKMP (Fig. 4B) in the MPXV-Zaire 79 genome.

Expression plasmid amplification

The plasmid was amplified by transformation of DH5α competent cells (Invitrogen) on LB-Ampicillin agar plates at 37°C for 24 hr. Isolated colonies were selected for overnight growth in LB-Ampicillin broth at 37°C with shaking at 225 rpm. The bacterial cells were collected and plasmid DNA isolated using the Wizard® *Plus* Midipreps kit (Promega, WI) according to the manufacturer's instructions. A restriction enzyme digest with XmaI (New England BioLabs, MA) was conducted at 37°C overnight and 65°C for 20 min. A DNA gel (0.7% agarose) electrophoresis run at 105V for 45 min confirmed proper plasmid amplification based on the size of the resulting band fragments. The final concentration of plasmid DNA was determined by optical density reading in a ND-1000 Spectrophotometer (NanoDrop®, DE).

Recombination with MPXV-Zaire 79

Parental MPXV strain Zaire 79 was obtained from the Centers for Disease Control and previously propagated in MA-104 cells. A confluent monolayer of VERO-E6 cells was prepared in EMEM (Gibco, NY) + 2.5% heat inactivated fetal bovine serum (FBS - Gibco) and

FIGURE 4. INSERTION OF FLUORESCENT GENES INTO MPXV-ZAIRE 79.
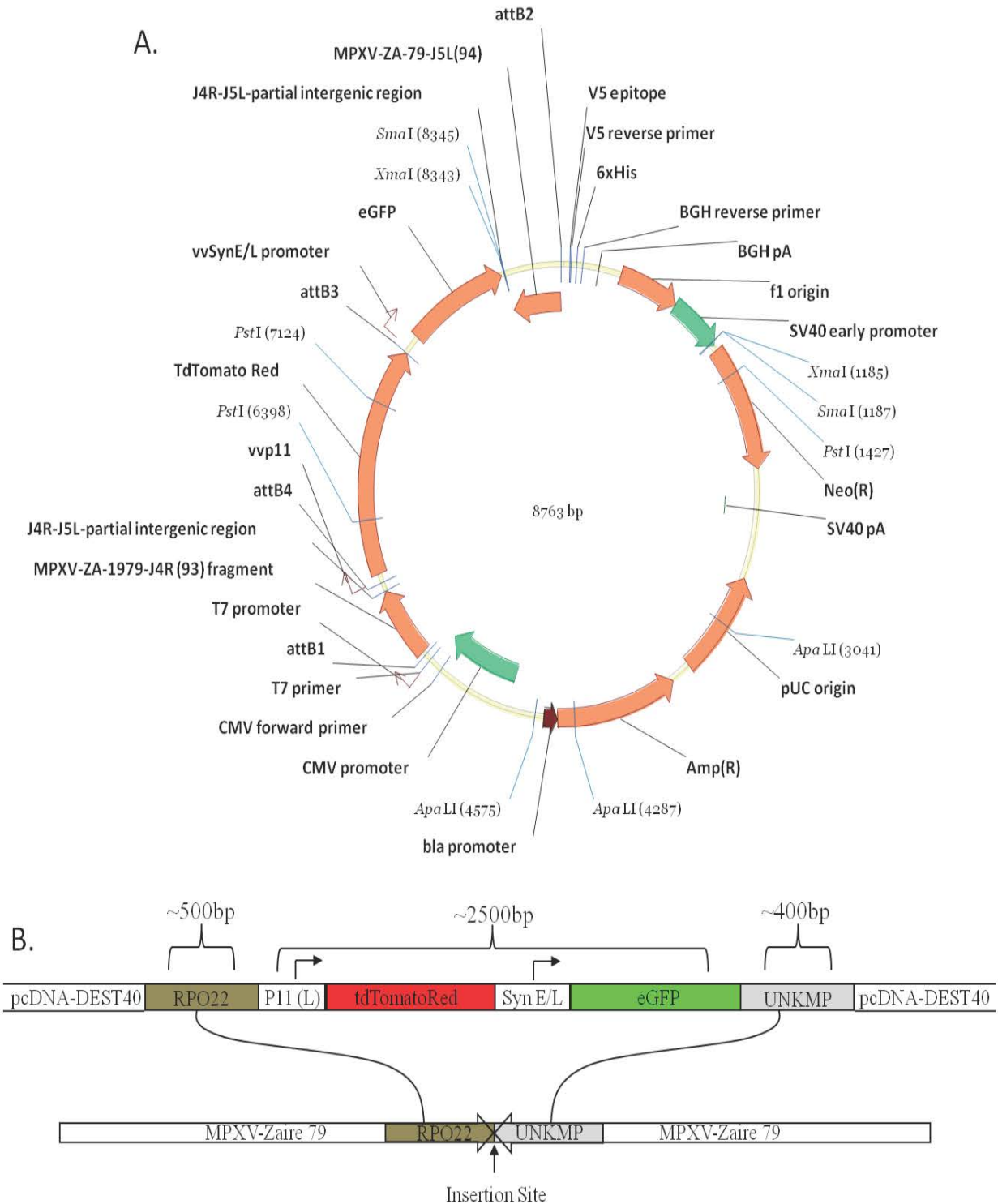Schematic representation of the expression plasmid pcDNA-DEST40 (A) and insertion sites of the fluorescent genes into the MPXV-Zaire 79 genome (B). The fluorescent genes and their viral promoters were inserted into the intergenic region between the RPO22 and UNKMP genes. The insertion plasmid and plasmid diagram were generously provided by Dr. Grant McFadden.

24

subsequently infected with parental MPXV (MOI=1) at 37ºC and 5% CO_2. Following 1 hr of absorption, the infection medium was removed and the cells washed with fresh Opti-MEM medium (Gibco). Plasmid DNA (2µg) was transfected into the cells using Lipofectamine™ 2000 (Invitrogen) in Opti-MEM medium according to manufacturer's instructions. The transfection medium was removed after 5 hr, fresh medium (EMEM + 2.5% FBS) was added, and the cells were incubated at 37ºC and 5% CO_2 for 24 hr. The cells were harvested into 1 mL of medium (EMEM + 2.5% FBS) and stored at -80°C for plaque purification assays.

Plaque purification assay

Harvested cells were lysed by 3 cycles of freeze/thaw and 3 rounds of sonication/vortex (15 s each). Fresh Vero-E6 cells were prepared in 6-well plates and incubated with 200 µL of the cell lysate at 37ºC and 5% CO_2. After 1 hr of absorption, the infection medium was removed and the cells washed and layered with a 2% low melting point (LMP - Promega) agarose-medium mixture (equal volume). Following incubation at 37ºC and 5% CO_2, the cells were scanned after 24 and 48 hr for fluorescence, and images collected using a fluorescent microscope. Plaques that contained both green and red fluorescence were collected with glass Pasteur pipettes and stored in 200 µL of medium (EMEM + 2.5% FBS). Each collected sample was lysed as described above using the same freeze/thaw and sonication/vortex cycles. Serial dilutions were made, plated onto confluent Vero-E6 cells and layered with the LMP agarose-medium mixture for another round of plaque picks. This process was repeated 4 times to ensure the generation of a uniform virus population in all dilutions.

Step-wise virus propagation and working stock generation

Once a uniform virus population was confirmed through fluorescence microscopy, a step-wise propagation of a virus stock was conducted. 250 µL of the final plaque pick was added to a

single well of confluent Vero-E6 cells in a 12-well culture plate. The infection was absorbed for 1 hr, followed by washing and the addition of fresh medium (EMEM + 2.5% FBS). 48 hr post-infection, the cells were harvested, freeze/thawed (x3), and sonicated/vortexed (x3), and 500 µL were added to a single well of confluent Vero-E6 cells in a 6-well culture plate. Infection and imaging were performed as described above. This process was repeated (with adjusted volumes) for T75 and T150 flasks of MA-104 cells; the cell pellet generated from the T150 infection was resuspended in 11 mL of medium, and 1ml was stored at -80°C. The remaining 10 mL was used to infect 5 confluent T-150 flasks of MA-104 cells (2 mL/flask). The infection was absorbed for 30 min, followed by the addition of 30 mL of fresh medium. All 5 flasks were harvested into a single 50ml conical tube 4 days post-infection. The cells were centrifuged at 400xg for 7 min, all but 2 mL of supernatant were removed which were used to resuspend the cell pellet. The cells were lysed, brought to a final volume of 5.5 mL with fresh medium (EMEM + 2.5% FBS) and aliquots of 500 µL were generated. One vial was used for PCR analysis, virus titer determination (plaque assay) and fluorescence uniformity testing (microscopy).

Once the virus seed stock was titered and determined to be a pure population through PCR and sequencing analysis (as described below), large scale propagation was conducted to generate a working stock. Twenty confluent T-150 flasks of MA-104 cells were infected with 1×10^{7} plaque forming units (pfu)/flask. The cells were harvested 4 days post-infection and combined into 2 conical tubes. The cell pellets were resuspended in 2 mL of medium (EMEM + 2.5% FBS) and lysed. The lysates were combined and brought to a final volume of 20 mL with medium. Aliquots of 500 µL were made and a small portion was set aside for virus titer determination and fluorescence uniformity testing.

Fluorescence microscopy

Fluorescent images were taken using a Nikon Eclipse te2000-s (Nikon Instruments INC., NY) equipped with a SPOT™ RT Monochrome camera (SPOT Imaging Solutions, MI) and processed with SPOT™ Advanced version 4.0.9 (SPOT Imaging Solutions). All images were collected using a 4x objective and laser exposure times were conserved across samples for each time point. eGFP images were collected using a GFP/FITC filter cube which contained band-pass (BP) excitation filter 490/20 and BP emission filter 525/36. tdTR images were collected using a RFP filter cube which contained BP excitation filter 555/25 and BP emission filter 605/52. The raw image files were processed and overlaid using Photoshop CS2 software (Adobe, CA).

Plaque assay

All samples (virus stocks, inocula, experimental samples) were titered using the following assay. Each sample was serially diluted to extend between the ranges of 10^{-1} and 10^{-12}. Fully confluent VERO-E6 cell monolayers were prepared in 6-well plates with subcomplete medium (EMEM + 1% Glutamine + 2% Heat Inactivated FBS). The medium was removed from the cell culture wells and 500 µL of each dilution was added in duplicate per well. The plates were incubated at 37°C and 5% CO_2 with gentle rocking every 15 min. The infection medium was removed after 1 hr; the cell layers were washed, and replaced with fresh subcomplete medium. The medium was removed 4 days post-infection, and 500 µL of a previously prepared crystal violet solution (1.3g Crystal Violet - Sigma-Aldrich, MO, 50 mL 200 proof Ethanol – Sigma-Aldrich, 650 mL deionized water, 300 mL 10% Neutral Buffered Formalin – Sigma-Aldrich) was added to each well. Following 20 min of staining, the crystal violet was removed and the plates rinsed with water. Once dry, the plaques were enumerated, the counts adjusted based on dilution factors and final titers were calculated.

PCR

Inactivation of samples and extraction of viral DNA were conducted using components from a QIAmp DNA Blood Mini Kit (Qiagen, CA). Samples were combined with a reagent mixture (PBS + Buffer AL + Protease Solution) at a 1:3 ratio and incubated for 1 hr at 56°C.

DNA extraction was conducted for each inactivated sample through the addition of 200 μL of 100% ethanol; samples were vortexed for 15 s and centrifuged at 8,000 rpm for 15 s. The mixture was added to a QIAmp spin column, centrifuged at 8,000 rpm for 60 s, and washed with Buffer AW1 and Buffer AW2 (Qiagen). The spin columns were placed into sterile collection tubes and 100 μL of elution buffer was added. The samples were kept at room temperature for 5 min and centrifuged at 8,000 rpm for 60 s. Samples were stored at -20°C until ready for use.

Quantitative real time polymerase chain reaction (RT-PCR) assays were conducted on extracted DNA samples based on the techniques previously established by (37) for viral genome quantification. The *pan*-orthopoxvirus detection probes targeted the hemagglutinin (HA) gene J7R using the TaqMan-MGB (Invitrogen) assay and was used to determine viral genome levels in the nonhuman primate study. To confirm a pure seed and working stock MPXV-GFP-tdTR population, a *pan*-orthopox, specific monkeypox (targeted F3L), cowpox (N3R), and vaccinia virus (A25L) probes were utilized. Previously prepared MGB master mix was combined with Platinum Taq Polymerase (Invitrogen). 15 μL of the mixture was combined with 5 μL of extracted DNA, run on a LightCycler 2.0 (Roche, IN) and analyzed using LightCycler Software Ver. 4.0 (Roche).

Sequencing

Primers were designed for PCR amplification of the insertion site following seed stock generation. 2 primer sets were used: P1 forward 5'-CCG CAA TAA CAT GGT AAC TGG AGT AG-3', P1 reverse 3'-GTG TTG TAG CTC CTG CCG TCG-5' and P2 forward 5'-GCA TGG ACG AGC TGT ACA AGT AAC AA-3', P2 reverse 3'-TTT CTC CGA CCA TTG TTG CGT AGC (Invitrogen). Following amplification, the gene products were sequenced using a GS FLX+ 454 system (Roche). Sequences were compared using SeqMan II software (DNASTAR, WI).

Growth curves

Growth curve experiments were conducted to compare the growth kinetics of the MPXV-GFP-tdTR to MPXV-Zaire 79 and MPXV-GFP. Fully confluent Vero-E6 cells in 6-well plates were infected (in triplicate) at MOI=5 with each virus type. The infection medium was absorbed at 37ºC and 5% CO_2. For the collection of time point T_0, the infection medium was immediately removed, fresh medium (EMEM + 2.5% FBS) was added and the cells harvested through gentle scraping. For all other time points (T_4, T_{12}, T_{24} and T_{48}), the infection medium was removed after 1 hr, the cells were washed, and fresh medium (EMEM + 2.5% FBS) was added. The collection of all time points included the centrifugation of the harvested cells, the removal of all but 200 μL of the supernatant and the storage of the cell pellet at -80°C. Once all time points were collected, the cells were lysed (as previously discussed) and prepared for plaque assay analysis.

Time course expression of eGFP vs. tdTR

A time course experiment was conducted to assess the expression patterns for both green and red fluorescence signals. Vero-E6 cells were prepared in 15 mL polypropelene tubes and infected at MOI=10 in suspension with mock, MPXV-GFP, and MPXV-GFP-tdTR. The cells were kept at constant low level shaking and incubated at 37ºC with 5% CO_2. 150,000 – 200,000 cells (250 μL) were collected from each tube at various time points (T_0, T_2, T_3, T_6, T_9, T_{12}, T_{24}

and T_{48}). The samples were washed with Pharmingen Stain Buffer (BSA – BD, CA), and centrifuged at 800 rpm for 5 min. The supernatant was removed, the cells fixed with 100µl of 4% paraformaldehyde (BDCytofix™ - BD), and held at 4°C. Once all the time points were collected (from the same vial), the cells were washed with 500 µL of stain buffer, and centrifuged at 800 rpm for 5 min (x2). The cells were resuspended in a final volume of 500 µL of stain buffer and run on a C6 flow cytometer (Accuri[®], NJ). Results were analyzed using CFlow[®] software (Accuri).

Ara-C treatment

Cytosine β-D-arabinofuranoside (Ara-C, Sigma-Aldrich) is a compound that inhibits DNA replication. A dilution of the stock sample was made to equal 50µg/mL in subcomplete medium (EMEM + 1% Glutamine + 2% Heat Inactivated FBS). Fully confluent Vero-E6 cells in 6-well plates were incubated at 37ºC and 5% CO_2 with 1 mL of Ara-C only, medium only, virus only (MOI=5), or Ara-C + virus (MOI=5). The incubation/infection medium was removed after 1 hr and fresh subcomplete medium (with and without Ara-C) was added. Fluorescent images were collected 24 and 48 hr post-infection.

Interferon-βeta Treatment of Monkeypox Virus Infections

The methods described in this section were previously published in "*In vitro* inhibition of monkeypox virus production and spread by Interferon-β" *Virology Journal* 2012 (34). The inclusion of the methods have been cleared for use in this thesis with approval from Dr. Sara Johnston (primary author) and BioMed Central Ltd (publishing company). [(Clearance Letters)]

My scientific contributions towards the manuscript included the generation/characterization of MPXV-GFP-tdTR (as described above), scientific study design for use of the virus (personal

communications with Dr. Johnston), technical support for the subsequent experiments involving MPXV-GFP-tdTR (set up of infections, collection of time points, execution of plaque assays), and the collection of fluorescence data (microscopy images, fluorescence analysis). I also wrote portions of the methods and results sections of the manuscript pertaining to the generation and characterization of MPXV-GFP-tdTR, generated figures for the MPXV-GFP-tdTR characterization experiments, and assisted with data analysis/interpretation for the generation of additional figures using MPXV-GFP-tdTR.

Interferon-βeta treatment

IFN-β (PBL InterferonSource, NJ) was titrated in HeLa (ATCC, VA) with pre-treatment 24 hr prior to infection with MPXV. The cells were infected at MOI=5 in the presence or absence of IFN-β for 1 hr. The infection medium was removed, the cells were washed and replaced with fresh medium (EMEM + 2.5% FBS) with or without IFN-β. The cells were harvested and viral titers calculated by plaque assay (as previously described).

Growth curve experiments were used to evaluate growth kinetics during treatment with 2000 U/mL of IFN-β. Confluent HeLa cells were treated or untreated with IFN-β (24 hr) and infected at MOI=5 or 0.01. The infection medium was removed after 1 hr, cells washed, and fresh medium (+/- IFN-β) was added. Fresh IFN-β was added to each well every 24 hr. The cells and supernatant were harvested separately at specific time points: MOI=5 (0, 24, 48, 72, and 96) hr post-infection and MOI=0.01 (0, 4, 12, 24, and 48) hr post-infection. The collection of T_0 was conducted slightly different in that the infection was immediately removed, cells washed and harvested. The titers were determined through plaque assay.

Fluorescence microscopy

HeLa cells were prepared and treated with or without 2000 U/mL of IFN-β for 24 hr. VA-9 and VN36 cells (Dr. Otto Haller, University of Freiburg, Germany) were left untreated. All cell populations were infected at MOI=5 with MPXV-GFP-tdTR and visualized through the use of a fluorescence microscope (as previously described) 24 hr post-infection. Relative fluorescence was determined through the use of a SpectraMax Gemini EM Fluorescence Microplate Reader (Molecular Devices, CA).

Intratracheal (IT) Infection of Nonhuman Primates

The following section details the methods and study design for the infection of three nonhuman primates with MPXV-GFP-tdTR using an intratracheal exposure route. I wrote the animal use protocol, designed/scheduled the experiments, collected all the data (physical observations and laboratory assays), and generated all of the figures. The techniques and basic study design were based on the experience I gained through my scientific contributions on the publication "A novel respiratory model of infection with monkeypox virus in cynomolgus macaques" *Journal of Virology*, 2011 (24).

Plaque reduction neutralization test (PRNT)

To ensure all animals were seronegative for monkeypox virus, blood was collected in serum separator vacutainer (BD) tubes 7 days prior to infection, centrifuged at 2,200 rpm for 10 min, and serum collected into a fresh tube. Each sample was held at 56°C for 30-45 min to inactivate any complement proteins. Serial dilutions were made in fresh subcomplete medium (EMEM + 1% Glutamine + 2% Heat Inactivated FBS). MPXV-Zaire 79 prepared as described above was diluted to 50pfu/well. The virus preparation was added to each sample and was incubated at 37°C and 5% CO_2 for 15 min. 100 μL of each mixture was added to fully confluent Vero-E6 cells in 6-well plates in duplicate, incubated at 37°C and 5% CO_2 for 1 hr, and brought

to a final volume of 2 mL with fresh subcomplete medium. The plates were kept at 37°C and 5% CO_2 for 4 days, followed by staining with crystal violet for plaque count assessment (as previously described).

Virus inoculum preparation and infection

Working stock vials of MPXV-GFP-tdTR were removed from -80°C storage and thawed at 37°C. The virus was sonicated/vortexed for three rounds, diluted in sterile PBS to create a concentration of $8x10^7$ pfu/mL, and kept on ice until the animals were ready for infection. A microsprayer with attached high pressure syringe (Penn-Century Inc., PA) was fitted into the working channel of a bronchoscope (PENTAX, NJ). Animals were anesthetized according to weight with telazol (Fort Dodge, IA) administered intramuscularly, and infected with 100 μL of inoculum deposited directly above the bifurcation of the trachea. Samples of the stock virus, inoculum, and an aliquot of the infection spray were retained for back titer analysis by plaque assay.

Animal husbandry and observations

Three male cynomolgus macaques (*Macaca fascicularis)* seronegative for monkeypox virus weighing 6.9, 7.0 and 7.9 kg were transferred from an onsite primate colony facility into a BSL-3+ laboratory suite and animal room located within USAMRIID one week prior to infection to allow proper acclimation. Animals were given access to water *ad libitum* and were fed 10 biscuits per day (2050 Primate Diet – Harlan Laboratories, MD) (changed daily) to monitor food consumption in regards to disease progression. Research was conducted under an IACUC approved protocol in compliance with the Animal Welfare Act, PHS Policy, and other Federal statutes and regulations relating to animals and experiments involving animals. The facility where this research was conducted is accredited by the Association for Assessment and

Accreditation of Laboratory Animal Care, International and adheres to principles stated in the Guide for the Care and Use of Laboratory Animals, National Research Council, 2011.

Animals were observed twice daily for 22 days post-infection. Observations every 2 days following anesthesia (as described above) included changes in weight, rectal temperature, nutritional consumption, behavior, and physical appearance. Dyspnea scoring and cough frequency were monitored as a measure of lung involvement. Lymphadenopathy was detected through physical manipulation of the inguinal and axillary lymph nodes. Scoring was conducted by assigning a numerical value, 0-3 according to severity. Lymphadenopathy was scored based on the diameter (in mm) of the lymph node: 0= <3; 1= 3-9; 2=≥10-19; 3= ≥20. Dyspnea was scored based on changes in observed breathing patterns: 0=normal breathing; 1= mildly labored; 2= labored; 3=marked labored breathing. Lesion development was tracked throughout the course of disease and enumerated according to body location. Physical manipulations were conducted under anesthesia every other day.

Sample collection

Blood (4 mL) was collected from the femoral artery of each animal following anesthesia in EDTA vacutainer (BD) tubes every 2 days following infection for virus genome quantification and clinical chemistry analysis. An AcT 10 (Beckman Coulter, CA) analyzer was used to measure white blood cell, red blood cell and platelet levels from EDTA whole blood. Virus genome levels were determined using RT-PCR on samples extracted and inactivated from whole blood (as described above).

Full necropsies were conducted and tissues collected following humane euthanasia with Fatal Plus Solution (Vortech Pharmaceuticals, MI) and exsanguination at the completion of the

animal study. Necropsies (I assisted with sample collection) and immunohistochemistry (IHC) staining were conducted by a board certified Veterinary Pathologist. Tissues were embedded in paraffin and analyzed by IHC. Following deparaffinization and peroxidase blocking, samples were stained with a rabbit polyclonal anti-pox specific antibody at room temperature for 1 hr. The samples were rinsed and incubated with a secondary antibody (a peroxidase-labeled polymer) for 30 min at room temperature. The sample slides were rinsed, a substrate-chomogen solution was added for 5 min, followed by a second rinse and staining with hematoxylin.

Results

A portion of the results presented in this section was previously published (34). Presentation of the results have been cleared for use in this thesis with approval from Dr. Sara Johnston (primary author) and BioMed Central Ltd (publishing company). A percent breakdown of my contribution towards the experimental conceptualization, data analysis, and figure generation for each previously published figure is presented in the figure legend. I designed the experiments, collected the results, and generated all the figures for the sections detailing the characterization of the double recombinant virus and the IT infection of nonhuman primates.

Characterization of MPXV-GFP-tdTR

Fluorescence microscopy confirmed the proper insertion of eGFP and tdTR into the MPXV-Zaire 79 genome to create MPXV-GFP-tdTR. An example of even color distribution was seen in a plaque 48 hr post-infection (Fig. 5). eGFP expression (Fig. 5A) and tdTR expression (Fig. 5B) were quantified individually, and an overlay of both images (Fig. 5C) was created. There was a zone of clearance, which was indicative of normal plaque formation, and there was uniform color distribution within each infected cell. This type of fluorescence distribution represents the standard used for all virus uniformity assessments.

Proper color uniformity was assessed at every step of the virus propagation and working stock generation experiments. Viral genome titers (genomes/mL) were determined based on the amplification of the specific sequences per detection probe. The RT-PCR results acquired from using the MPXV specific probe (F3L) and the *pan*-orthopoxvirus probe (J7R) demonstrated equal levels of viral genome detection, which validated the use of the *pan*-orthopox specific probe for the detection of MPXV-GFP-tdTR by PCR in the IT NHP study. The use of cowpox

virus and vaccinia virus specific probes showed no contamination of either virus in the final

virus stocks. Sequencing of MPXV-GFP-tdTR demonstrated proper insertion of the fluorescent

genes between RPO22 and UNKMP.

The results of a one-step (high MOI) growth curve illustrate the similarities in growth

kinetics of MPXV-Zaire 79, MPXV-GFP and MPXV-GFP-tdTR (Fig. 5D), each reaching 10^8

pfu/mL by 24 hr post-infection. The sustained viral titers *in vitro* demonstrate a lack of

attenuation due to the incorporation of the fluorescent gene inserts.

A time course experiment was used to further characterize the timing and frequency of

late gene expression *in vitro*. The fluorescence profile of MPXV-GFP was compared to the

double recombinant MPXV-GFP-tdTR. Both viruses contained the same early gene promoter for

expression of eGFP. The analysis entailed the flow cytometric collection of 10,000 single cell

population events gated on forward and side scatter properties for each time point. eGFP

expression was compared to tdTR (late protein) expression by directly comparing the number of

cells positive for each fluorescence signal (Fig. 6). Gates were generated based on negative

fluorescence as seen in the mock infected control group. Samples were compensated to ensure

eGFP signal would not carry over into the tdTR channel.

eGFP expression from MPXV-GFP infected cells (Fig. 6A) was seen as early as 2 hr

post-infection (found in 5.5% of cells), and the number of eGFP positive cells increased quickly

through the time points, reaching near maximum levels by 24 hr (93.3% of cells). eGFP signal

from MPXV-GFP-tdTR infected cells was also detected at 2 hr post-infection (Fig. 6B) at similar

levels (3.7% of cells). The number of cells expressing eGFP increased steadily, though at a
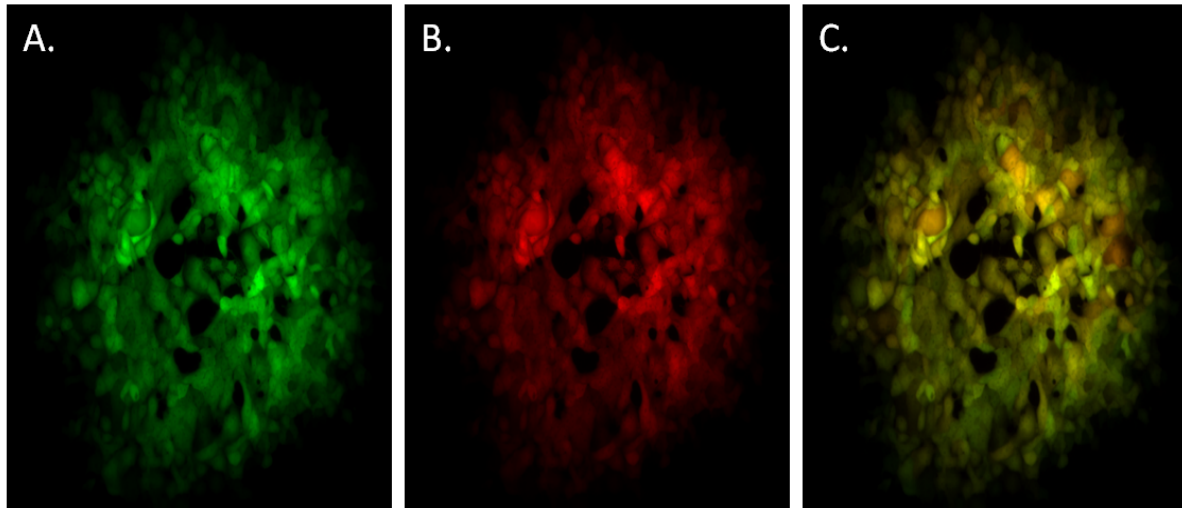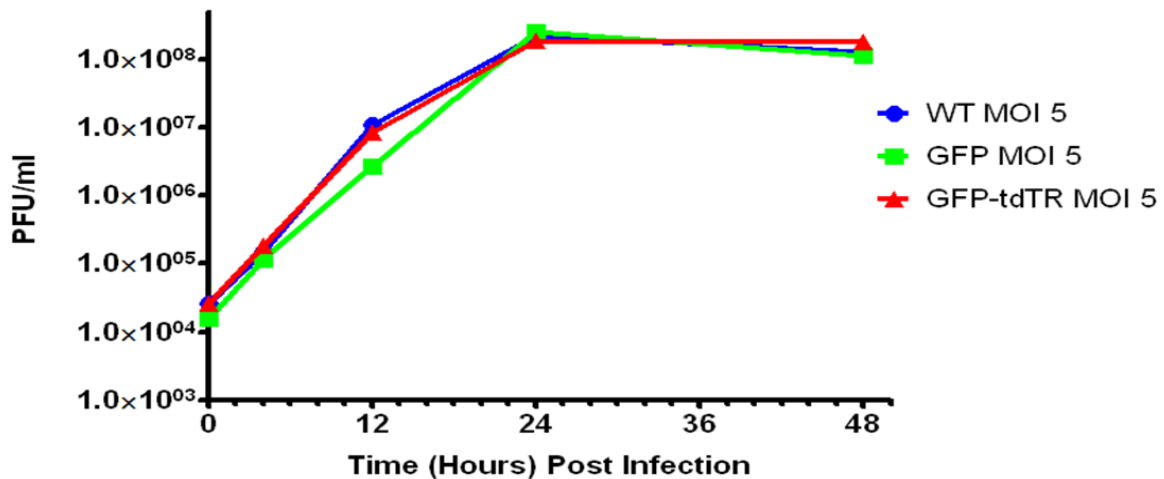
FIGURE 5. FLUORESCENT MICROSCOPY OF MPXV-GFP-TDTR AND GROWTH CURVE ANALYSIS.
Fluorescent images of a plaque 48 h.p.i. in Vero-E6 cells (A) eGFP expression, (B) tdTR expression, (C) overlay of both images. (D) Growth curve results (in triplicate) comparing MPXV-Zaire 79 (WT), MPXV-GFP and MPXV-GFP-tdTR in Vero-E6 cells infected at MOI=5. Results demonstrated no attenuation in either recombinant virus. I conducted 100% of the experimental conceptualization/data collection/figure generation. Portions of the figure appear in the published manuscript (34 - Fig. 1A).
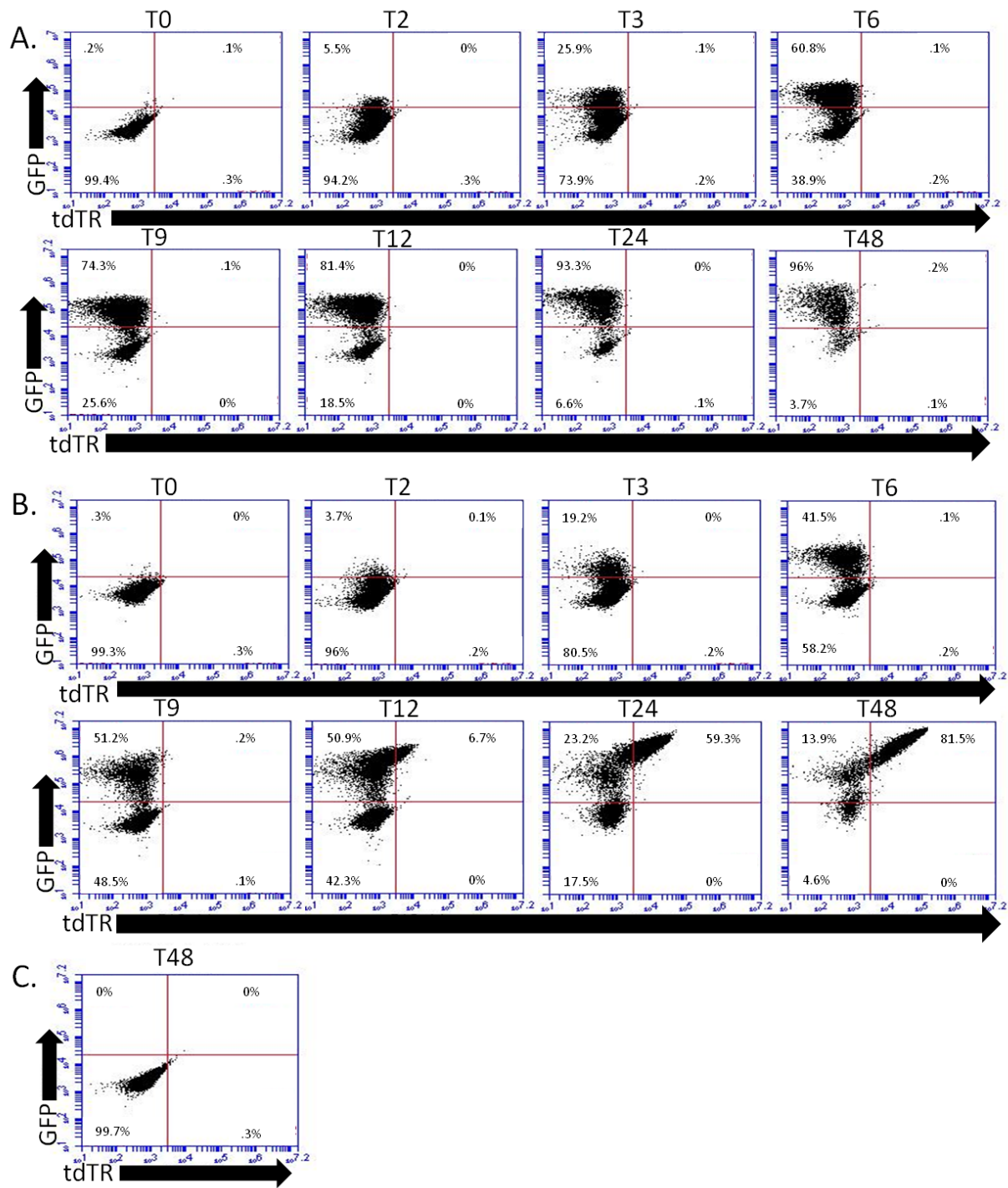
FIGURE 6. EXPRESSION PROFILE CHARACTERIZATION.
Flow cytometry results comparing eGFP expression and tdTR expression in Vero-E6 cells infected at MOI=10 with (A) MPXV-GFP, (B) MPXV-GFP-tdTR, or (C) Mock. X-axis represents the number of cells with tdTR fluorescence, the Y-axis represents the number of cells with eGFP fluorescence. Each plot represents 10,000 single cell events and demonstrates a quantifiable difference in the expression profile between the two viruses. I conducted 100% of the experimental conceptualization/data collection/figure generation.

slightly slower rate, and tdTR expression began between 9 and 12 hr post-infection as depicted by the cells that were double-positive (upper right quadrant). By 24 hr, 82.5% of the total cells contained eGFP signal, while 59.3% of the total cells were positive for both eGFP and tdTR. By 48 hr post-infection, the combined total fluorescence of the MPXV-GFP-tdTR infection (95.4% of total cells) matched the number of fluorescent cells in the MPXV-GFP infection (96.2% of total cells); an indication that even though the expression of eGFP was slightly reduced early in infection, the double recombinant virus was still able to reach maximum levels of fluorescence saturation by 48 hr post-infection. The results demonstrated a clear expression profile of a productive infection, where 81.5% of the total cells were double-positive for eGFP and tdTR.

Ara-C has been extensively used to prevent the expression of late gene proteins and inhibit viral replication (8, 63). Here Ara-C was used to further confirm the correlation of tdTR fluorescence with late gene expression. The use of 50µg of Ara-C per mL produced a complete inhibition of late gene expression as evidenced by the lack of any tdTR expression (Fig. 7). Multiple images were collected at 24 and 48 hr post-infection per field including bright field, eGFP signal, and tdTR signal. The contrast in the level of late gene signal was seen when treated samples (Fig. 7A and 7C) were compared to virus only controls (Fig. 7B and 7D). A lack of cellular toxicity was demonstrated at these time points with the inclusion of bright field images (Fig. 7E and 7F) of cells treated with Ara-C alone. Since it was shown that eGFP expression occurred very early in the infection process, its expression profile was not dependent upon virus replication. This was further demonstrated in Figure 7B and 7D where eGFP positive cells were still present at 24 and 48 hr post-infection in the presence of Ara-C.
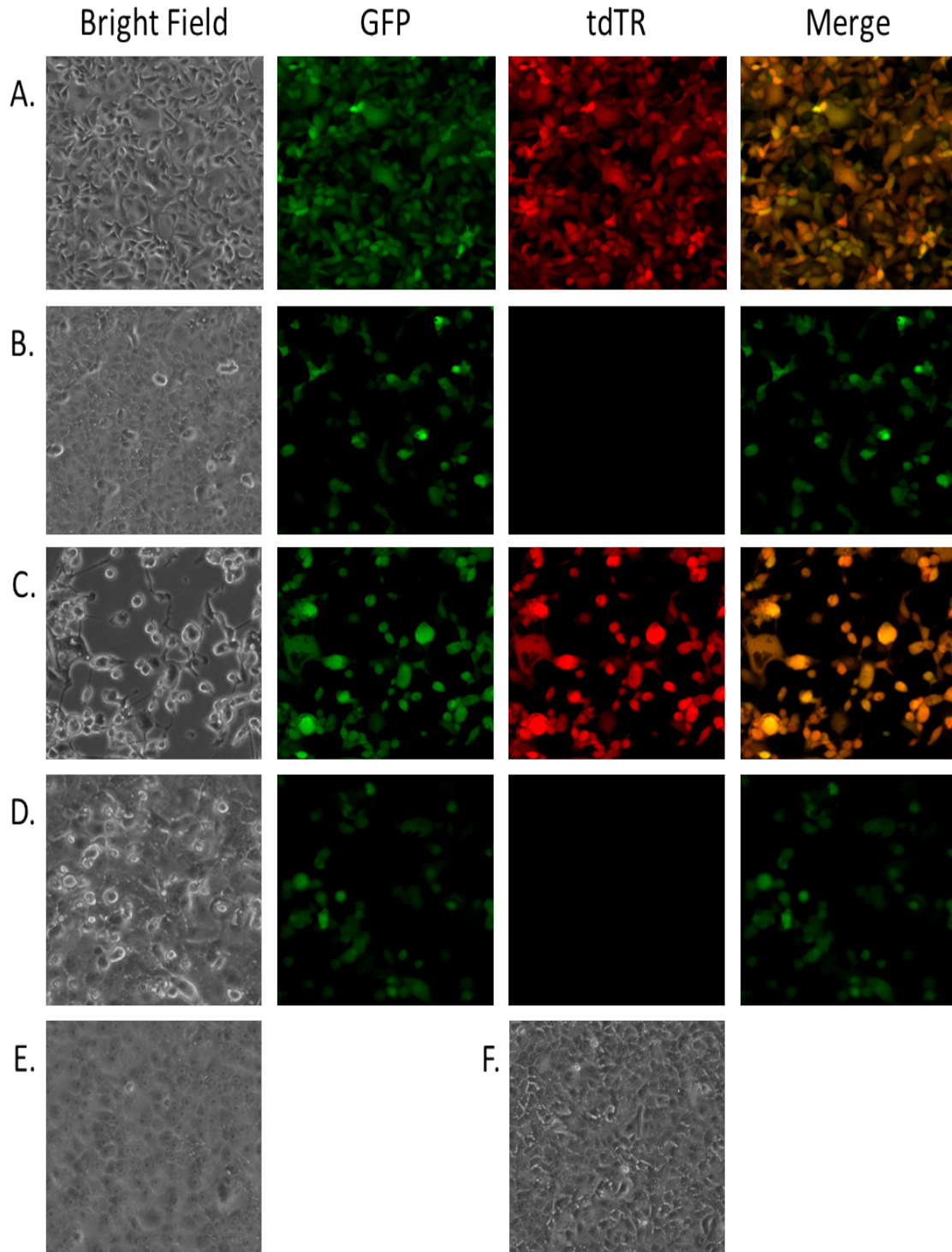
FIGURE 7. ARA-C TREATMENT OF MPXV-GFP-TDTR INFECTION.
Fluorescent microscopy images of Vero-E6 cells infected at MOI=5 demonstrated a link between tdTR color and late gene expression. (A) Virus only 24 h.p.i, (B) Ara-C + Virus 24 h.p.i., (C) Virus only 48 h.p.i., (D) Ara-C + Virus 48 h.p.i. Bright field images of Ara-C only (E) 24 h.p.i. and (F) 48 h.p.i. I conducted 100% of the experimental conceptualization/data collection/figure generation. Portions of the figure appear in the published manuscript (34 - Fig. 1B).

IFN-β Treatment of MPXV-GFP-tdTR Infections

IFN-β treatment titration was conducted using HeLa cells and MPXV-Zaire 79. 2000 U/mL was determined to be the optimum, nontoxic concentration to use as demonstrated by the 91% reduction in viable virus 24 hr post-infection (manuscript Fig. 1A). HeLa cells pretreated with 2000 U/mL of IFN-β for 24 hr were infected with MPXV at either a low (0.01) or high (5) MOI, and virus titers in the cells were determined by plaque assay. The results of the virus titers for each time point of the growth curves (Fig. 8) illustrate the reduction in the amount of viable virus isolated at specific time points. In the low MOI growth curve (Fig. 8A), there was a marked decrease in the amount of cell associated virus between 48 and 72 hr post-infection. Viral levels in treated samples reached the same level as untreated controls by 120 hr post-infection; however, a clear attenuation of cell to cell spread was evident in the presence of IFN-β. In the high MOI growth curve (Fig. 8B), there was a half-log difference in viral titers within the first 12 hr. By 24 hr, this difference had increased to a full log, demonstrating an inhibition of virus production.

Fluorescent microscopy images of HeLa cells untreated or pretreated with IFN-β and infected with MPXV-GFP-tdTR collected 24 hr post-infection (Fig. 9) demonstrate a difference in expression profiles. Normal viral gene expression patterns in untreated cells (top row Fig. 9A) compared to reduced expression patterns of both GFP and tdTR signals (bottom row Fig. 9A) demonstrate the effect of IFN-β treatment. There was an equal reduction of relative fluorescence (as measured by a fluorescence microplate reader) for both colors (Fig. 9B), indicating that viral inhibition was occurring at a step prior to early gene expression.
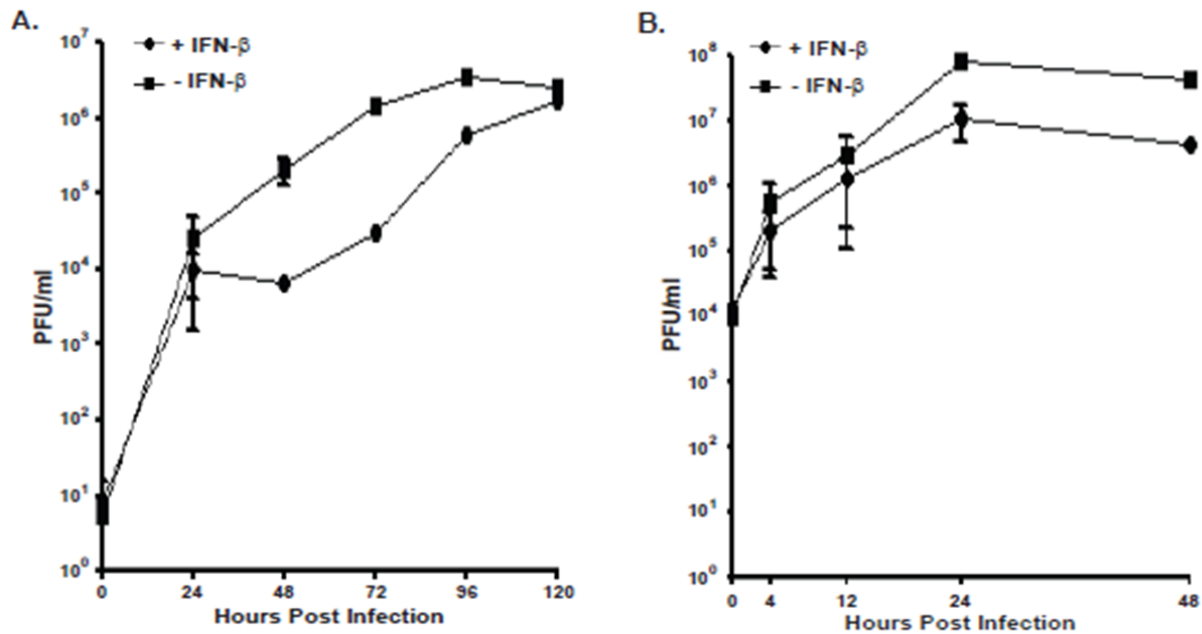
FIGURE 8. IFN-B TREATMENT OF HELA CELLS INFECTED WITH MPXV-ZAIRE 79.

Growth curves of HeLa cells treated (♦) or untreated (■) with IFN-β. The graphs represent viral titers determined through plaque assay from cells infected at MOI=0.01 (A) or MOI=5 (B) with MPXV-Zaire 79. (A) Growth curves that demonstrate a reduction in cell to cell viral spread as a result of IFN-β treatment. (B) Growth patterns that illustrate a reduction in viable virus production as a result of IFN-β treatment. I conducted 25% of the experimental conceptualization and 25% of the data collection. This figure was compiled by obtaining graphs (generated by Dr. Johnston) that appear in the published manuscript (34 - Fig. 1B & 4A).
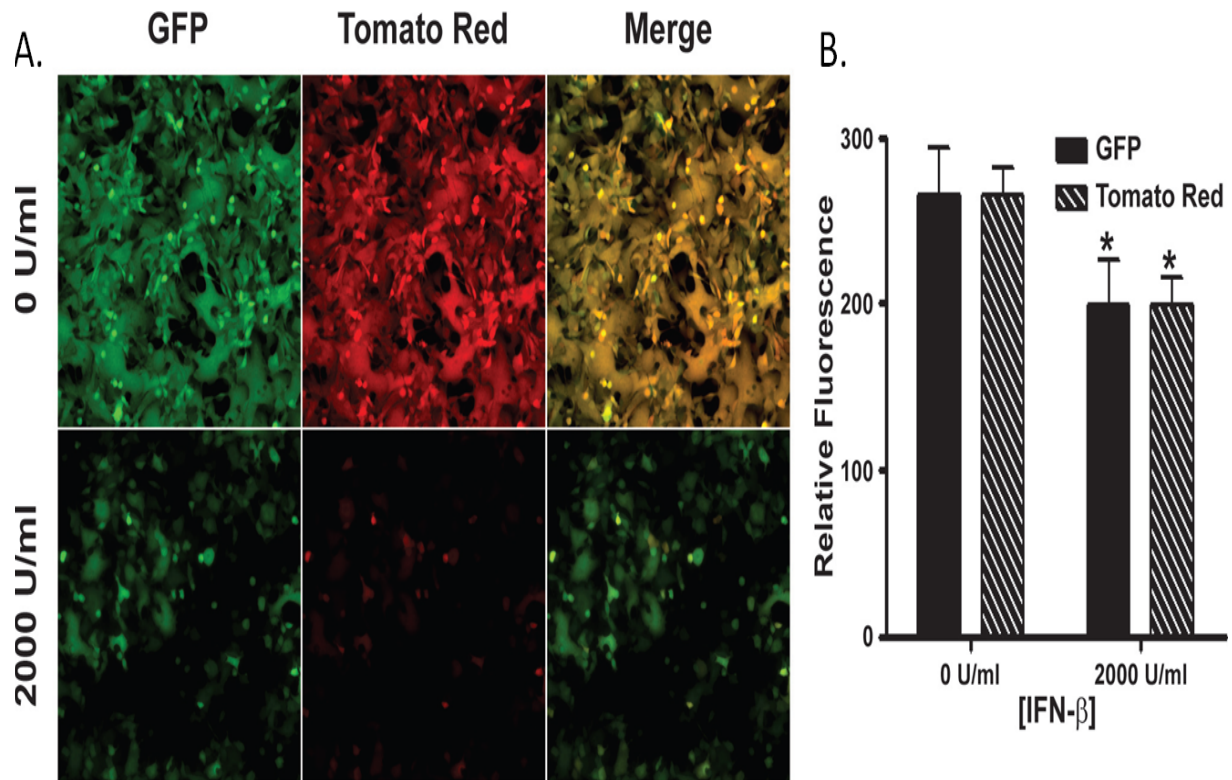
FIGURE 9. IFN-B TREATMENT OF MPXV-GFP-TDTR INFECTION.
(A) Fluorescent microscopy images taken 24 h.p.i. of treated (2000 U/mL) or untreated (0 U/mL) HeLa cells infected at MOI=5 with MPXV-GFP-tdTR. (B) Relative fluorescence of each expression color determined using a fluorescence microplate reader. Treatment resulted in reduced expression of both fluorescent genes. I conducted 50% of the experimental conceptualization and 50% of the data collection. This figure was generated by Dr. Johnston and appears in the published manuscript (34 - Fig. 3).

In this paper, it was shown that MxA expression was induced by IFN-β and co-localized with the viral protein A33 at the site of membrane wrapping during morphogenesis in the presence of MPXV infection (34). To determine what effect MxA had on MPXV infection, VN36 (control cell line) and VA-9 (constitutively express MxA) cells (as previously described in (20)) were infected with either MPXV-Zaire 79 or MPXV-GFP-tdTR at MOI=5; and viral reduction was assessed 24 hr post-infection (Fig. 10). A comparison of viral titers through plaque assay indicated a roughly 91% reduction in the amount of cell associated viable virus in VA-9 cells compared to VN36 cells (Fig. 10A). Fluorescence microscopy using MPXV-GFP-tdTR revealed an equal reduction in both GFP and tdTR expression 24 hr post-infection in VA-9 cells as compared to VN36 cells. The results, shown here as fluorescent microscopy images (Fig. 10B) and relative fluorescence measurements (Fig. 10C), indicated that MxA inhibitory effects occurred prior to early gene expression.
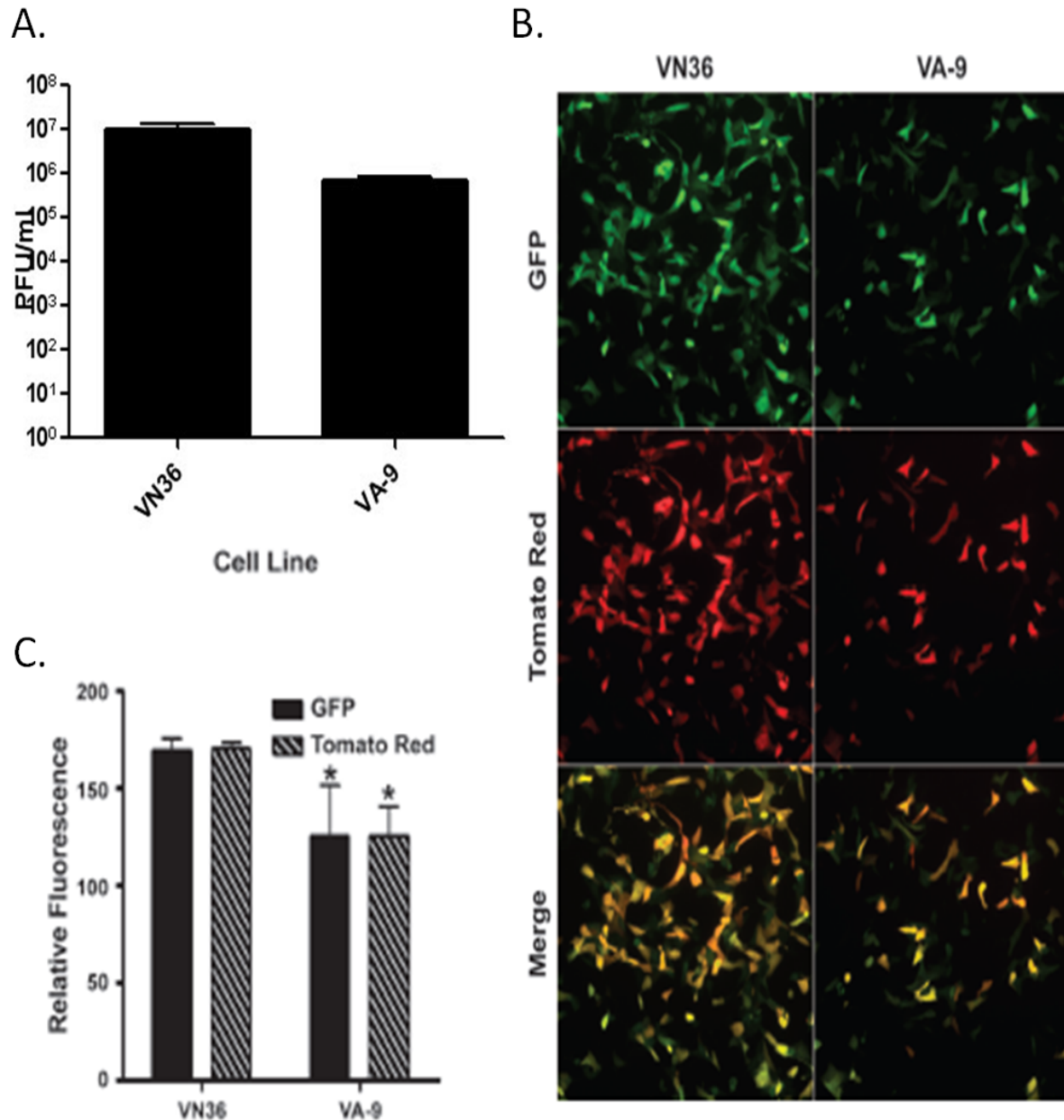
FIGURE 10. INFECTION OF VN36 AND VA-9 CELLS WITH MPXV-ZAIRE 79 OR MPXV-GFP-TDTR.
(A) Comparison of viral titers (pfu/mL) in VA-9 and VN36 cells 24 h.p.i. Cells were infected with MPXV-Zaire 79 at MOI=5. The difference represents a 91% reduction in the production of infectious virus in the presence of MxA (constitutively expressed by VA-9 cells). (B) Fluorescent microscopy images of MPXV-GFP-tdTR infected cells (MOI=5) comparing levels of early and late gene expression (eGFP and tdTR) 24 h.p.i. (C) Relative fluorescence of each expression color determined using a fluorescence microplate reader. Treatment resulted in reduced expression of both fluorescent genes. I conducted 50% of the experimental conceptualization and 50% of the data collection. This figure was generated by Dr. Johnston and portions appear in the published manuscript (34 - Fig. 7B).

Intratracheal Infection of Nonhuman Primates with MPXV-GFP-tdTR

A study was conducted using MPXV-GFP-tdTR in conjunction with the IT infection model to evaluate its virulence and assess its ability to mimic human disease. Three animals were challenged with 2.75×10^7 pfu of virus using the same techniques described in the IT manuscript (24). All three animals survived challenge, though each exhibited clinical manifestations of monkeypox disease similar to surviving animals in the original IT model development study (24). All animals developed classical lesions (Fig. 11) as seen in previous NHP models of MPXV infection. Images were collected on day 14 post-infection of animal #1 (which experienced the highest disease severity). Two types of monkeypox lesions (Fig. 11A) were seen on the head of the animal: a scabbed lesion with classical crust-like features (the white arrow), and a desquamating lesion that has begun to resolve (the black arrow). Ulcerative lesions were observed on the tongue (Fig. 11B) and other aspects of the oral mucosa. Pustular lesions were seen on the palms of the hands (Fig. 11C) and the soles of the feet. Prominent axillary lymphadenopathy (Fig. 11D) and inguinal lymphadenopathy were observed in all three animals.

Peripheral viral blood titers, as determined by PCR analysis ranged from $10^5 - 10^6$ genomes/mL at the height of disease severity, D8 – D10 post-infection (Fig. 12A). The number of lesions observed ranged from $100 - 325$ (Fig. 12B). There was a direct correlation between the number of lesions enumerated and the level of viral genomes in the blood. Animal 1 had the highest viral titers, lesion count, and more severe disease as determined through clinical observations and scoring. Animal 2 however, only developed viremia 1 log above detection and had the fewest lesions. Lesions in all three animals began to desquamate between D12 - D16 post-infection. All lesions were resolved by the end of the study and at the time of necropsy.
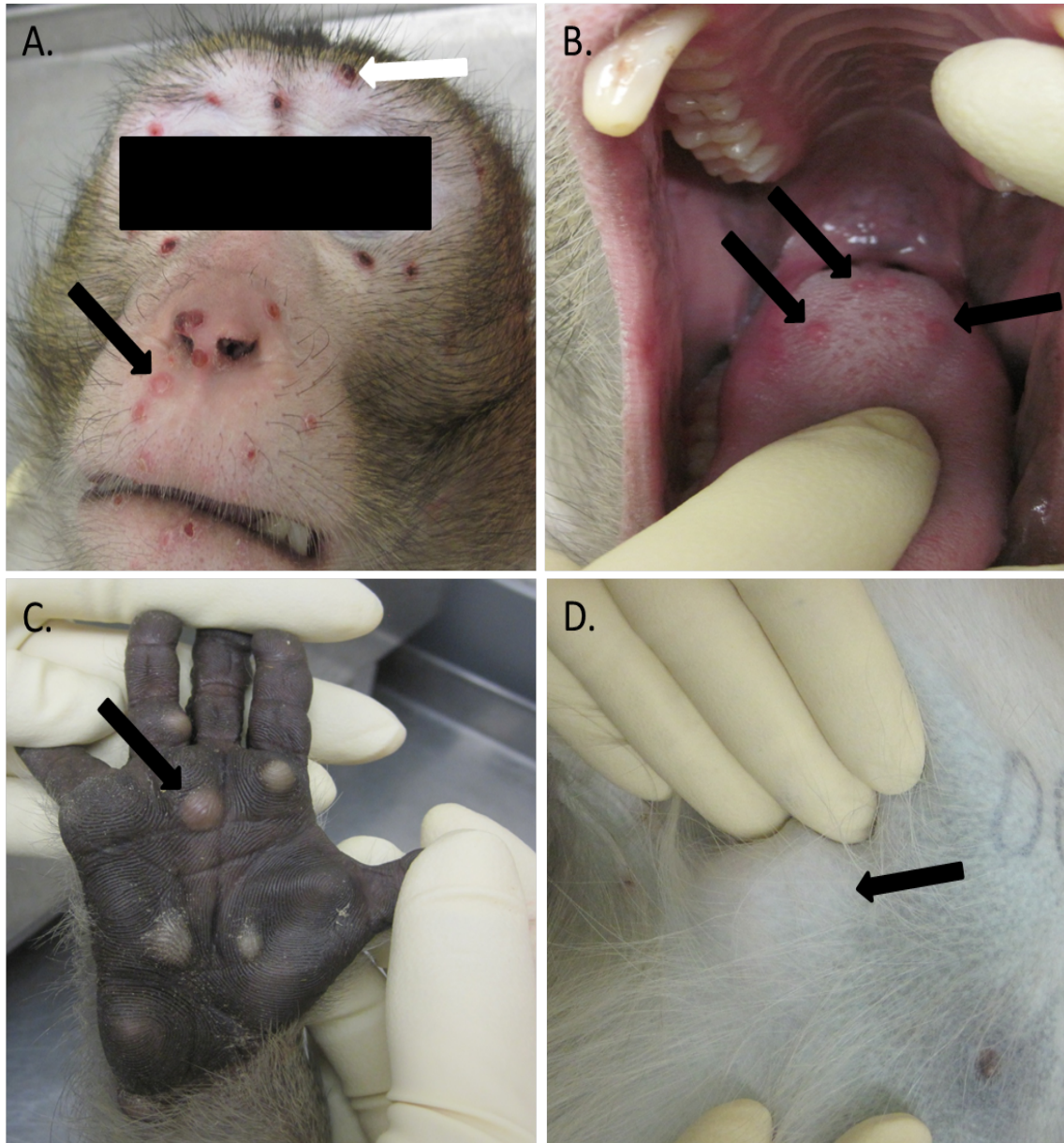
FIGURE 11. IMAGES OF NHPS INFECTED WITH MPXV-GFP-TDTR D14 POST-INFECTION.
Animals developed classical disease symptoms (lesion progression and lymphadenopathy) as previously characterized in (24). (A) Examples of a scabbed lesion (white arrow) and a desquamating lesion (black arrow) shown on the face of an animal on day 14. (B) Ulcerative lesions on the tongue. (C) Pustules located on the right palm. (D) Severe axillary lymphadenopathy.

Complete blood counts (CBC) were conducted on each sample collection day. The percent change as compared to baseline (D0) levels for each animal was calculated and graphed in Figure 13. In all 3 animals, white blood cell (WBC), red blood cell (RBC), and platelet (PLT) numbers fluctuated throughout disease course. WBC and PLT levels peaked on D10 and D12 post-infection in each animal (Fig. 13A and 13C). Animals 2 and 3 had inconsistent spikes in RBC levels, but saw an overall reduction by D12 post-infection; whereas animal 1 had a progressive reduction in RBC levels through D12 (Fig. 13B). All three animals returned to baseline levels in the three analytes by D18, which correlated with recovery from disease. There was an abnormal RBC reading associated with animal 1 on D22, which was the end of study terminal bleed. The animal was fully recovered and the observed value was a probable outlier not related to disease, though no control animals (uninfected) were used in parallel for this study. Histopathology indicated enlarged lymph nodes and spleen that correlated to lymphoid hyperplasia with draining inflammatory cells in response to infection. Immunohistochemical staining of isolated tissues were negative for viral presence as a result of all three animals fully recovering from infection prior to necropsy.
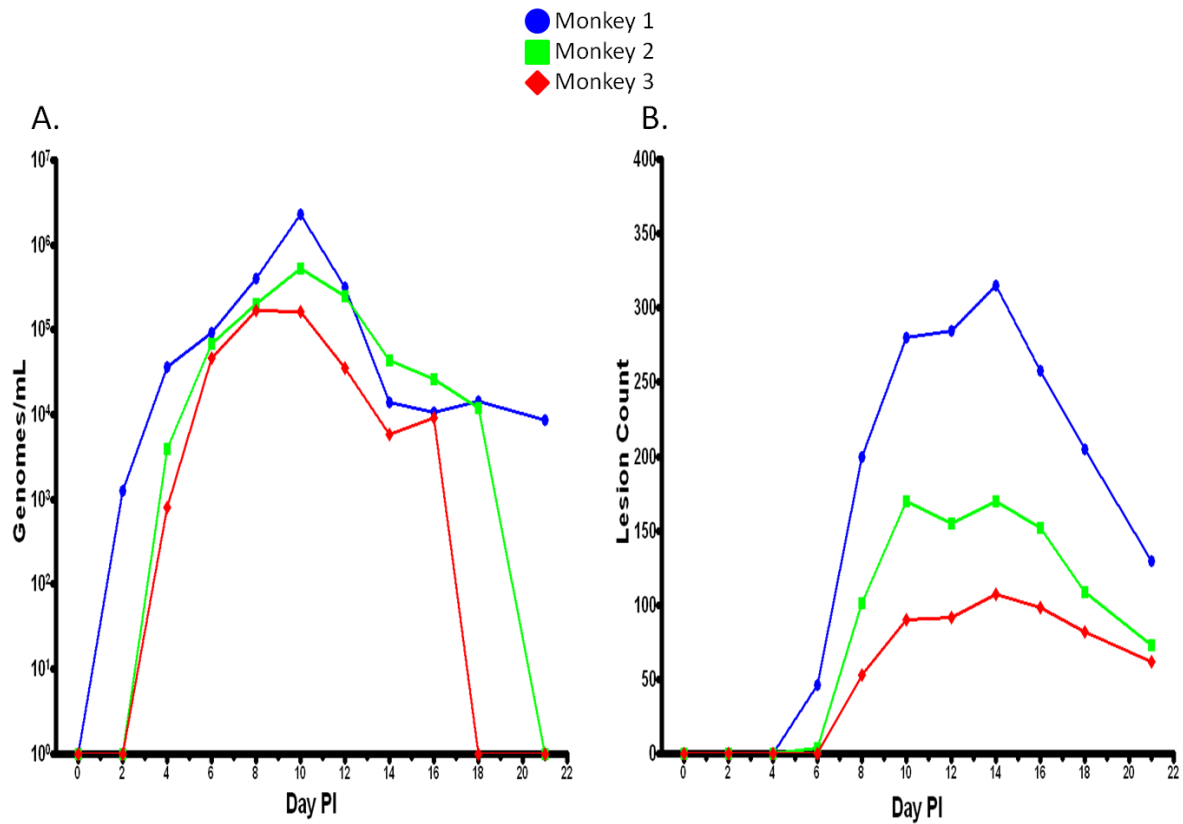
FIGURE 12. VIRUS TITERS AND LESION COUNTS OF NHPS INFECTED WITH MPXV-GFP-TDTR.
Animals reached blood virus titers and lesion count numbers similar to the surviving animals previously characterized in (24). Samples were collected and observations recorded every 2 d.p.i. (A) Blood virus titers (genomes/mL) for each animal throughout disease course – peak values at D10 p.i. per animal. (B) Lesion counts per animal, peak numbers D12 p.i. per animal.
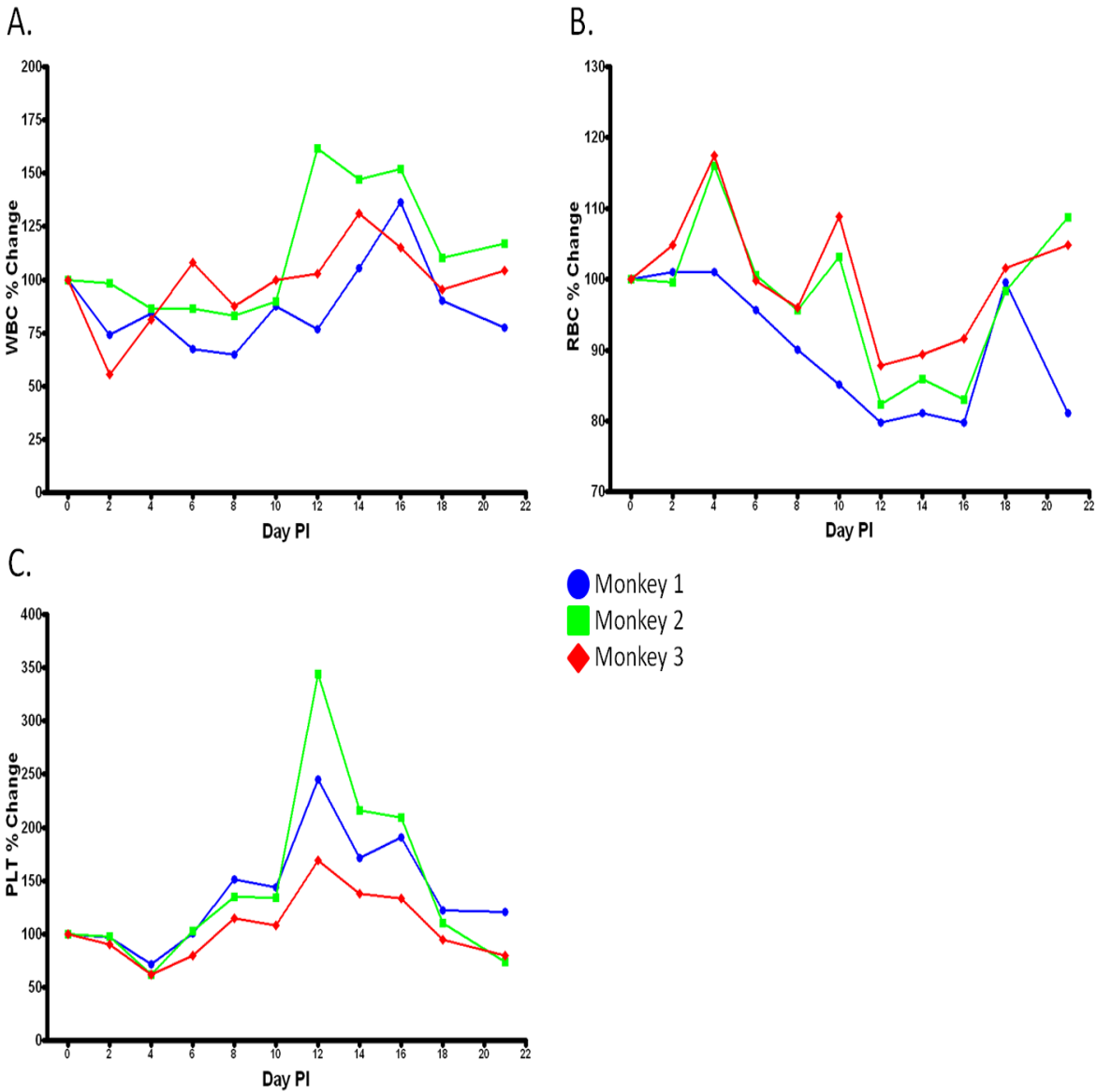
FIGURE 13. CHANGES IN BLOOD ANALYTES IN NHPS INFECTED WITH MPXV-GFP-TDTR.
Blood samples were collected every 2 d.p.i. and analyzed for complete blood counts (CBC). Percent change in cell counts are shown for (A) White blood cells, (B) Red blood cells, and (C) Platelets. Animals exhibited changes in CBC similar to the surviving animals previously characterized in (24).

Discussion

Though an effective vaccine exists for smallpox and monkeypox, there are limitations to the use of this vaccine due to its reactogenicity. With the cessation of an active vaccination program and waning herd immunity, a large susceptible population has emerged worldwide. The currently licensed vaccine utilizes live vaccinia virus (VACV) which can cause severe adverse reactions in individuals who are immunocompromised (HIV infection, radiation therapy, chemotherapy, etc.) or have skin conditions (psoriasis or eczema) (45). Therefore, a large portion of the susceptible population would be ineligible to receive vaccination. Concurrent with the development of new vaccine candidates (DNA subunit), there has been a push to develop post-exposure therapeutic strategies that could be implemented in quick response to potential orthopoxvirus threats (36).

The generation and utilization of fluorescent viruses can have a profound impact on therapeutic testing and evaluation. Recombinant VACV that express fluorescent proteins at multiple stages during virus infection have been used in rapid high content analysis for therapeutic screening (17). Potential new compounds were tested using a 96-well plate infection format, and fluorescence expression was quantified using a fluorescence plate reader (16). One such screen yielded the identification of a novel pyridopyrimidinone compound (CMLDBU6128) that exhibits broad-spectrum antiviral activity against multiple orthopoxviruses including MPXV *in vitro* (16). This nonnucleoside analog was shown to block intermediate and late gene expression, which led to the inhibition of viral replication (16).

VACV is the most highly studied orthopoxvirus due to its ease of use under BSL-2 conditions. Although VACV and MPXV are very similar, *in vitro* growth kinetics and *in vivo*

pathogenesis are significantly different. For VACV in A549 cells, early gene expression occurs 2 hr post-infection and late gene expression 4 hr post-infection (17). This is in contrast to the expression profile we have observed for MPXV-GFP-tdTR, where late gene expression does not occur until 9 hr post-infection. Due to differences in gene expression profiles, immunomodulatory proteins, and pathogenesis; it cannot be assumed that MPXV and VACV will respond in the same manner to the same treatment strategy (10, 13, 19, 36). Therefore, in order to demonstrate cross-protective action for newly identified therapeutics, drug evaluations should also be done using MPXV in order to reproduce the desired effects with a more pathogenic virus. Previously, a recombinant MPXV expressing eGFP from an early virus promoter was generated and characterized (22). eGFP expression was used to identify infected cells that were expressing early gene products. However, this virus provided little information about genome replication and subsequent late gene expression.

When testing a therapeutic against orthopoxviruses, it can be informative if both early and late protein production are assessed to determine the effectiveness of the therapeutic and to identify the possible mechanism of action. To this end, a MPXV that expressed eGFP from an early virus promoter and tdTR from a late virus promoter was generated in an effort to further our understanding of monkeypox disease and to better identify and test new therapeutics. Flow cytometric analysis revealed a fluorescent expression profile that could be assessed and quantified on a cell by cell basis. The data demonstrated a distinct advantage to using MPXV-GFP-tdTR when evaluating downstream viral activity in a particular cell population in the presence and absence of a therapeutic compound as evidenced by treatment with Ara-C.

Additional benefits from using MPXV-GFP-tdTR for therapeutic testing include the ability to quickly determine downstream effects using visualization techniques by using

53

fluorescence microscopy or fluorescence plate readers. Since eGFP signal is produced very early in infection, a lack or reduction in eGFP fluorescence intensity alone following treatment with an antibody or small molecule would demonstrate an inhibition of viral entry. An equal reduction in the levels of both eGFP and tdTR fluorescence would indicate that the therapeutic functions to block early events during infection (eg. entry, early gene transcription, etc.). Finally, a reduction of tdTR alone would suggest a block of late gene expression and subsequent morphogenesis, egress, and release. The use of MPXV-GFP-tdTR would provide a quick (within 24 hr) assessment of predicted viral output and provide initial insight into whether a block in replication occurred prior to or following late gene expression. A more in depth analysis of late gene expression can also be assessed by post-infection treatment with a therapeutic to determine if the compound can limit active late gene expression by preventing fluorescence signal increase over time. Utilizing this virus in conjunction with a rapid high throughput system such as a 96-well fluorescence plate reader would provide an efficient, multiplexed platform for drug screening. Since eGFP and tdTR expression are not directly linked to mature virion assembly, fluorescence analysis alone cannot be used to quantify viable virus production. Therefore, follow up experiments must still be performed that directly assess virus production and release such as plaque assays and growth curves.

In order to assess the usefulness of MPXV-GFP-tdTR for therapeutic development, we wanted to run a proof-of-concept study to test this virus in a system where MPXV inhibition had already been demonstrated. It had recently been shown by Dr. Sara Johnston (USAMRIID) that MPXV production was significantly reduced in the presence of IFN-β. In collaboration with her, we tested MPXV-GFP-tdTR in this system to provide supporting data for the study and to demonstrate the effectiveness of MPXV-GFP-tdTR for therapeutic testing. Using this virus, we

further characterized the inhibitory effects of IFN-β and examined a possible mechanism of action through the induction of MxA (data outlined in this report and presented in our recent publication (34)). Fluorescence and confocal microscopy performed using MPXV-GFP-tdTR demonstrated an equal reduction in both eGFP and tdTR expression following IFN-β treatment and MxA expression. Both results indicate that viral inhibition might occur early by either preventing infection or blocking the expression of early proteins. To date, the effects of IFN-β treatment on monkeypox infection *in vivo* have not been explored. On the basis of our data we were able to validate the use of MPXV-GFP-tdTR for the future evaluation of novel countermeasures against orthopoxviruses.

We were also able to show the *in vivo* application of MPXV-GFP-tdTR using a previously published IT model of monkeypox in cynomolgus macaques (24). The results of this study illustrated the ability of the recombinant virus to produce a classical monkeypox disease. Even though all animals survived infection, they each developed high viral blood titers, lesions, lymphadenopathy and respiratory complications. The reference points for each clinical symptom were determined based on the animals that survived challenge in our previously published manuscript (24). All the animals that survived to the end of their respective study experienced the same peak in disease severity between D8 and D10 post-infection. Comparative changes in CBC values were seen in overall RBC depletion, WBC fluctuations, and PLT spikes. Peak viral titers (10^6) and lesion counts (100-400) were observed by D10 in the surviving animals. We were able to validate the use of MPXV-GFP-tdTR for future *in vivo* studies designed to better characterize pathogenesis, immune cell involvement, and for therapeutic evaluation.

Further validation of this recombinant virus for animal use can be achieved through additional NHP studies that focus on specific infection patterns within circulating immune cells

throughout the disease course. Information regarding the immune cells that are preferentially infected *in vivo*, and changes that occur in the activation and functional states of these cells, would expand the current knowledge of monkeypox pathogenesis. One of the limitations in this line of experimentation has been the lack of an effective antibody assay for the detection of circulating infected cells *in vivo.* The use of MPXV-GFP-tdTR would allow for the evaluation of viral presence within specific subsets of immune cells and provide information on whether these cell populations support a productive infection.

As part of the original thesis research, preliminary experiments were conducted with isolated peripheral blood mononuclear cells (PBMC) from naïve NHPs and infected *in vitro* with either MPXV-GFP or MPXV-GFP-tdTR. In an attempt to determine if a particular subset of immune cells were preferentially targeted by MPXV, samples were stained with surface marker antibodies for immunophenotyping and infection frequency determination through flow cytometry. This experimentation was designed to compare the infection frequencies of specific immune cells *in vitro* to the infection frequencies observed *in vivo*; to determine if infection status correlated with pathogenesis. Preliminary results indicated monocytes as being preferentially infected, based on eGFP expression profiles using MPXV-GFP, which was observed in previously published studies using VACV *in vitro* (15, 54). Since eGFP expression alone did not provide information about virus replication, experiments using MPXV-GFP-tdTR were designed to identify cellular modulations that occur in monocyte derived cell types associated with late gene expression. The results were inconclusive and described in more detail in Appendix B.

Sequential sampling NHP studies using MPXV-GFP-tdTR would provide an opportunity for an in depth look at tissue specific infection profiles (specifically lymphoid tissues such as the

spleen, lymph nodes, and bone marrow). Determining which cell populations support productive infections would provide a better understanding of pathogenesis and could enhance the efficacy of drug evaluation. Having a platform to visualize inhibition of virus replication could provide a detection method for early therapeutic action. The collection of bronchoalveolar lavage (BAL) fluid during these studies could also be utilized to further examine the role of immune cells that are targeted early in infection. Following respiratory exposure, it is predicted that lung epithelium and aveolar macrophages are preferentially targeted and possibly provide a pathway for systemic dissemination (18). By sequentially collecting BAL and tissue samples throughout disease progression, tracking of viral dissemination can be performed.

Whole body fluorescent imaging of nonhuman primates infected with fluorescent viruses can be achieved with the proper excitation source and camera/filter combination (22, 23). Utilizing this visualization technique with MPXV-GFP-tdTR for therapeutic evaluation would provide real-time data to assess the likely effectiveness of treatment in visible areas (skin, oral cavity). This would allow for earlier identification of virus infection, which was described in (21) as fluorescent foci 2 days prior to lesion development. Foci that fail to express tdTR would provide preliminary information about virus replication in the absence of tissue samples for plaque assay and PCR. In addition, the progress of infection can be readily tracked without interfering with physical and clinical observations of an infected animal, a practice that cannot be achieved during a sequential sampling study.

In summary, smallpox and monkeypox remain viable biological threats given the increasing size of the susceptible population and the limitations of current vaccination strategies. Therefore, it is important that we work to develop and test post-exposure therapeutics. To fulfill the FDA animal rule, many animal models have been developed to replicate human disease. To

date, none of the available models of MPXV infection replicate all of the features of human

infection, although nonhuman primate models have come close. Here, I have discussed the

generation of a new recombinant MPXV that has been validated for the evaluation of an antiviral

therapeutic (IFN-β) and shown to exhibit some pathogenesis in NHPs (IT exposure route). The

data strongly support the future use of this virus in animal model and therapeutic development

studies.

Appendix A

Additional manuscript contributions.

The following material was generated from five animal studies involving BALB/c mice infected with Rift Valley Fever Virus and will appear in greater detail in two manuscripts currently submitted or in preparation:

1. Brian M. Friedrich, **Kenny Lin**, John Langford, Spencer Stonier, Louis Altamura, Gene Olinger, and Darci R. Smith, *Aerosolized Rift Valley Fever Virus Exposure Causes a Significant Difference in the Chemotactic and Inflammatory Gene Expression Response in the Murine Model* (**In Preparation**).

    <u>Scientific contributions:</u>

    My contributions were primarily through technical laboratory support in isolating, preparing, and staining samples of PBMCs and spleens for flow cytometric and mRNA analysis from 170 animals. I was involved with the design, analysis, and preparation of the written portions (methods, results and analysis) for the flow cytometry data. I was also involved in the discussions with Dr. Smith (corresponding author and study director) that lead to the publication ready organization of the cytokine and chemokine mRNA gene expression results.

2. Christopher Reed, **Kenny Lin**, Catherine Wilhelmsen, Brian Friedrich, Ashley Keeney, Ginger Donnelly, Joshua Shamblin, and Darci R. Smith, *Aerosolized Rift Valley Fever Virus Causes Earlier and More Severe Neuropathology in the Murine Model, which has Important Implications for Therapeutic Development* (**Submitted, PLOS NTD**).

Scientific contributions:

My contributions were primarily through technical laboratory support and through multiple discussions with Dr. Smith (corresponding author and study director) about the inclusion, exclusion, and organization of the results for publication.

Rift Valley Fever Virus (RVFV) is a zoonotic bunyavirus in the *Phlebovirus* genus that infects livestock and humans throughout Sub-Saharan Africa and Egypt. Mosquito species (*Aedes* and *Culex*) are the predominant vectors responsible for primary infections, though contact (aerosol exposure) with infected biological materials has also been implicated. RVFV infection in humans usually presents as headache, myalgia, fever, and in certain cases (~1%) retinitis, hepatitis, encephalitis, hemorrhage, and even death. RVFV poses a biological threat because the vector species is distributed globally, the virus is highly infectious as an aerosol, and an outbreak can have devastating effects on a region's livestock. Current treatment strategies include supportive therapy and the limited use of ribavirin. The development of representative animal models of disease progression is critical for therapeutic advancement. (47, 53)

Due to the scope and number of animals involved in the following studies, the technical work was divided amongst two working groups: those involved with animal handling, and those involved with sample processing. I worked solely within the sample processing group, and closely with the study director for experimental design, execution, and data analysis.

To further expand our understanding of disease pathogenesis, six- to eight-week old female BALB/c mice were infected with 1000 PFU of the ZH501 strain of RVFV either subcutaneously (SC) or through aerosol exposure. SC inoculations were performed with a volume of 100 μL of virus inoculum. Aerosol exposure was performed using a collision

nebulizer for 10 min. The study was divided into three experiments: the first was to monitor survival and collect biological samples following humane euthanasia when the animals were moribund D3 – D9 post-infection. The second was a serial sampling study, and the third was designed to evaluate the effect of ribavirin treatment on disease progression. Daily animal observations included changes in weight, temperature, natural behavior, physical appearance and activity.

Blood and tissues were collected for viral titer determination, histopathology, electron microscopy, blood chemistry and hematology analysis. White blood cells (WBC) were isolated from whole blood (collected at necropsy) and splenocytes for flow cytometry and miRNA expression assays. The flow cytometry staining panel included cell surface markers for immunophenotyping and the virus-specific antibody 4D4, which targeted the viral glycoprotein Gn on the cell surface. Changes in cytokine and chemokine mRNA gene expression profiles were characterized using the nCounter miRNA Expression Assay (nanoString Technologies, WA).

Based on the results, we concluded that there was no significant difference in mortality between the exposure routes; however, there were pathophysiological differences in disease progression. Animals infected through aerosol exposure exhibited more weight loss, higher levels of virus in the brain, more severe neuropathology, and greater changes in cytokine expression profiles. Animals infected SC had significantly more RVFV positive staining in circulating lymphocytes and monocytes as demonstrated by flow cytometry. Both routes of infection led to acute hepatitis, a reduction in lymphocytes, and an increase in liver enzymes and neutrophils. Preliminary cytokine and chemokine gene expression results suggested a modulation

of pro-inflammatory genes could be an early predictor for disease severity, though further analysis is required.

Post-exposure treatment with ribavirin was partially protective when animals were infected SC, but was not effective when animals were infected by aerosol exposure. Treatment of the SC group resulted in reduced weight loss, less fluctuations in temperature, and increased survival. Though treated animals infected by aerosol exposure exhibited the same disease progression as untreated animals, the mean time to death was extended by 3.5 days, indicating that treatment had some impact on disease progression. The exact mechanism of antiviral action of ribavirin on RVFV is not well understood, but a possible explanation for the differential effectiveness for SC and aerosol could be aggressive neural involvement associated with aerosol exposure and a limited ability of ribavirin to cross the blood-barrier. Therefore, ribavirin treatment would not be a recommend treatment strategy for aerosol exposure to RVFV.

In summary, our results demonstrated differences in RVF pathogenesis were associated with route of infection. The increased viral replication in the brain and subsequent encephalitis seen with aerosol exposure mimic the severest form of human RVF disease. The differences in disease and response to ribavirin treatment highlighted the importance of considering route of infection for the evaluation of therapeutics, and the increased need for better RVFV specific treatment strategies. More in-depth evaluation regarding immune cell infection frequencies, cytokine/chemokine modulations, and site of primary virus replication in relation to disease severity are being performed to further our understanding of these infection models.

Appendix B

Additional material not included in thesis.

One of the intended uses of the MPXV-GFP-tdTR strain was to test the hypothesis that monocyte derived cell types were preferentially targeted (in circulation) during monkeypox infections, and that subsequent changes in activation/maturation of the infected cells would correlate to changes in the pro-inflammatory cytokine profile, influencing disease progression. The first aim was to confirm monocytes as a preferentially targeted immune cell population. The second aim was to identify what cellular modulations (changes in activation and cytokine regulation) occurred in these monocyte populations associated with late gene expression. The third aim was to determine if *in vitro* changes correlated to disease progression seen in NHPs.

The first level of experimentation involved PBMCs isolated from NHPs, and their subsequent infection with MPXV-GFP *in vitro*. Preliminary immunophenotyping data of the mixed PBMCs showed CD14+ monocytes as a targeted cell population. The percentage of infected (GFP +) cells was less than 10% of the total cells, which was attributed to the low overall number of permissive cell types found in the non-homogenous population. As a result, several different strategies were implemented to increase the number of monocytes isolated from NHP EDTA blood prior to infection. These strategies included: magnetic bead separations (both positive and negative selection), cellular adhesion/separation through plating, blood centrifugal elutriation, and cellular sorting through flow cytometry (FACSAria II, BD). Due to the limitations associated with using NHP blood (low volume, restrictions on how frequent an animal can be bled, reagent cross-reactivity, animal variability, and overall cell numbers), none of the isolation techniques produced a high yield of pure, isolated monocytes. Therefore, many

of the downstream experiments (associated with aims two and three) failed to produce conclusive data. Complicated surface staining panels, low cell numbers, and improper antibody optimizations confounded the flow cytometry experiments designed to assess infected monocyte subpopulations and activation status. Furthermore, the low sample sizes did not yield a viable platform to properly assess changes in cytokine gene expression (mRNA analysis) or cytokine production (CBA analysis). I also attempted to obtain PBMCs from NHPs that were infected IT with MPXV-GFP-tdTR (see results section). Unfortunately, similar complications were encountered, severely limiting the amount of information obtained from the study. In addition to blood collections, bronchoalveolar lavage was also performed (every 4 days) on all three animals to determine if alveolar macrophages were a targeted early in infection. However, the volume and the number of viable cells collected were not enough to provide conclusive staining profiles or confirm viral presence.

Though the results were mostly inconclusive, I found some evidence that supported the hypothesis that monocytes are more readily infected than lymphocytes in NHPs infected with MPXV. Preliminary results suggested an arrest of viral replication at early gene expression in MPXV-GFP-tdTR infected monocytes, which was based on the inhibition of tdTR expression as evidenced through fluorescent microscopy and flow cytometry; however these experiments required further validation. To properly assess the role of monocytes in MPXV infections, these experiments need to be repeated with appropriate controls and optimizations. I would suggest the use of isolated human monocytes to remedy the complications of using immune cells isolated from NHPs for future *in vitro* experiments. However, doing so would limit the ability to correlate the results to an *in vivo* NHP disease system, which currently stands as the best surrogate for human monkeypox.

References

1. **Andrei, G., D. B. Gammon, P. Fiten, E. De Clercq, G. Opdenakker, R. Snoeck, and D. H. Evans.** 2006. Cidofovir resistance in vaccinia virus is linked to diminished virulence in mice. J Virol **80:**9391-9401.

2. **Artimo, P., M. Jonnalagedda, K. Arnold, D. Baratin, G. Csardi, E. de Castro, S. Duvaud, V. Flegel, A. Fortier, E. Gasteiger, A. Grosdidier, C. Hernandez, V. Ioannidis, D. Kuznetsov, R. Liechti, S. Moretti, K. Mostaguir, N. Redaschi, G. Rossier, I. Xenarios, and H. Stockinger.** ExPASy: SIB bioinformatics resource portal. Nucleic Acids Res **40:**W597-603.

3. **Berhanu, A., D. S. King, S. Mosier, R. Jordan, K. F. Jones, D. E. Hruby, and D. W. Grosenbach.** 2009. ST-246 inhibits in vivo poxvirus dissemination, virus shedding, and systemic disease manifestation. Antimicrobial agents and chemotherapy **53:**4999-5009.

4. **Bray, M., and M. Buller.** 2004. Looking back at smallpox. Clinical infectious diseases : an official publication of the Infectious Diseases Society of America **38:**882-889.

5. **Buller, R. M., and G. J. Palumbo.** 1991. Poxvirus pathogenesis. Microbiological reviews **55:**80-122.

6. **Chakrabarti, S., J. R. Sisler, and B. Moss.** 1997. Compact, synthetic, vaccinia virus early/late promoter for protein expression. BioTechniques **23:**1094-1097.

7. **Chapman, J. L., D. K. Nichols, M. J. Martinez, and J. W. Raymond.** 2010. Animal models of orthopoxvirus infection. Veterinary pathology **47:**852-870.

8. **Connor, J. D., L. Sweetman, S. Carey, M. A. Stuckey, and R. Buchanan.** 1974. Effect of adenosine deaminase upon the antiviral activity in vitro of adenine arabinoside for vaccinia virus. Antimicrobial agents and chemotherapy **6:**630-636.

9.   **Cosma, A., S. Buhler, R. Nagaraj, C. Staib, A. L. Hammarin, B. Wahren, F. D. Goebel, V. Erfle, and G. Sutter.** 2004. Neutralization assay using a modified vaccinia virus Ankara vector expressing the green fluorescent protein is a high-throughput method to monitor the humoral immune response against vaccinia virus. Clinical and diagnostic laboratory immunology **11:**406-410.

10.   **Damon, I. K.** 2011. Status of human monkeypox: clinical disease, epidemiology and research. Vaccine **29 Suppl 4:**D54-59.

11.   **Day, S. L., I. A. Ramshaw, A. J. Ramsay, and C. Ranasinghe.** 2008. Differential effects of the type I interferons alpha4, beta, and epsilon on antiviral activity and vaccine efficacy. Journal of immunology **180:**7158-7166.

12.   **de Swart, R. L., M. Ludlow, L. de Witte, Y. Yanagi, G. van Amerongen, S. McQuaid, S. Yuksel, T. B. Geijtenbeek, W. P. Duprex, and A. D. Osterhaus.** 2007. Predominant infection of CD150+ lymphocytes and dendritic cells during measles virus infection of macaques. PLoS pathogens **3:**e178.

13.   **Dembek, Z. F.** 2007. Medical aspects of biological warfare. Borden Institute Office of the Surgeon General United States Army Medical Dept. Center and School.

14.   **Di Giulio, D. B., and P. B. Eckburg.** 2004. Human monkeypox: an emerging zoonosis. The Lancet infectious diseases **4:**15-25.

15.   **Dominguez, J., M. M. Lorenzo, and R. Blasco.** 1998. Green fluorescent protein expressed by a recombinant vaccinia virus permits early detection of infected cells by flow cytometry. Journal of immunological methods **220:**115-121.

16.   **Dower, K., C. M. Filone, E. N. Hodges, Z. B. Bjornson, K. H. Rubins, L. E. Brown, S. Schaus, L. E. Hensley, and J. H. Connor.** 2012. Identification of a

pyridopyrimidinone inhibitor of orthopoxviruses from a diversity-oriented synthesis library. Journal of virology **86:**2632-2640.

17. **Dower, K., K. H. Rubins, L. E. Hensley, and J. H. Connor.** 2011. Development of Vaccinia reporter viruses for rapid, high content analysis of viral function at all stages of gene expression. Antiviral research **91:**72-80.

18. **Estep, R. D., I. Messaoudi, M. A. O'Connor, H. Li, J. Sprague, A. Barron, F. Engelmann, B. Yen, M. F. Powers, J. M. Jones, B. A. Robinson, B. U. Orzechowska, M. Manoharan, A. Legasse, S. Planer, J. Wilk, M. K. Axthelm, and S. W. Wong.** 2011. Deletion of the monkeypox virus inhibitor of complement enzymes locus impacts the adaptive immune response to monkeypox virus in a nonhuman primate model of infection. Journal of virology **85:**9527-9542.

19. **Fields, B. N., D. M. Knipe, and P. M. Howley.** 2007. Fields virology, 5th ed. Wolters Kluwer Health/Lippincott Williams & Wilkins, Philadelphia.

20. **Frese, M., G. Kochs, U. Meier-Dieter, J. Siebler, and O. Haller.** 1995. Human MxA protein inhibits tick-borne Thogoto virus but not Dhori virus. Journal of virology **69:**3904-3909.

21. **Fuller, T., H. A. Thomassen, P. M. Mulembakani, S. C. Johnston, J. O. Lloyd-Smith, N. K. Kisalu, T. K. Lutete, S. Blumberg, J. N. Fair, N. D. Wolfe, R. L. Shongo, P. Formenty, H. Meyer, L. L. Wright, J. J. Muyembe, W. Buermann, S. S. Saatchi, E. Okitolonda, L. Hensley, T. B. Smith, and A. W. Rimoin.** 2011. Using remote sensing to map the risk of human monkeypox virus in the Congo Basin. EcoHealth **8:**14-25.

22.   **Goff, A., E. Mucker, J. Raymond, R. Fisher, M. Bray, L. Hensley, and J. Paragas.**
2011. Infection of cynomolgus macaques with a recombinant monkeypox virus encoding
green fluorescent protein. Archives of virology **156:**1877-1881.

23.   **Goff, A., N. Twenhafel, A. Garrison, E. Mucker, J. Lawler, and J. Paragas.** 2007. In
vivo imaging of cidofovir treatment of cowpox virus infection. Virus research **128:**88-98.

24.   **Goff, A. J., J. Chapman, C. Foster, C. Wlazlowski, J. Shamblin, K. Lin, N.
Kreiselmeier, E. Mucker, J. Paragas, J. Lawler, and L. Hensley.** 2011. A novel
respiratory model of infection with monkeypox virus in cynomolgus macaques. Journal
of virology **85:**4898-4909.

25.   **Golden, J. W., and J. W. Hooper.** 2008. Heterogeneity in the A33 protein impacts the
cross-protective efficacy of a candidate smallpox DNA vaccine. Virology **377:**19-29.

26.   **Haller, O., S. Gao, A. von der Malsburg, O. Daumke, and G. Kochs.** 2010. Dynamin-
like MxA GTPase: structural insights into oligomerization and implications for antiviral
activity. The Journal of biological chemistry **285:**28419-28424.

27.   **Handley, L., R. M. Buller, S. E. Frey, C. Bellone, and S. Parker.** 2009. The new
ACAM2000 vaccine and other therapies to control orthopoxvirus outbreaks and bioterror
attacks. Expert Rev Vaccines **8:**841-850.

28.   **Hooper, J. W., E. Thompson, C. Wilhelmsen, M. Zimmerman, M. A. Ichou, S. E.
Steffen, C. S. Schmaljohn, A. L. Schmaljohn, and P. B. Jahrling.** 2004. Smallpox
DNA vaccine protects nonhuman primates against lethal monkeypox. Journal of virology
78:4433-4443.

29.   **Hudson, P. N., J. Self, S. Weiss, Z. Braden, Y. Xiao, N. M. Girgis, G. Emerson, C.
Hughes, S. A. Sammons, S. N. Isaacs, I. K. Damon, and V. A. Olson.** 2012.

Elucidating the role of the complement control protein in monkeypox pathogenicity. PloS one **7:**e35086.

30. **Huggins, J., A. Goff, L. Hensley, E. Mucker, J. Shamblin, C. Wlazlowski, W. Johnson, J. Chapman, T. Larsen, N. Twenhafel, K. Karem, I. K. Damon, C. M. Byrd, T. C. Bolken, R. Jordan, and D. Hruby.** 2009. Nonhuman primates are protected from smallpox virus or monkeypox virus challenges by the antiviral drug ST-246. Antimicrobial agents and chemotherapy **53:**2620-2625.

31. **Huggins, J. W.** 2012. Personal Communication.

32. **Jahrling, P. B., L. E. Hensley, M. J. Martinez, J. W. Leduc, K. H. Rubins, D. A. Relman, and J. W. Huggins.** 2004. Exploring the potential of variola virus infection of cynomolgus macaques as a model for human smallpox. Proceedings of the National Academy of Sciences of the United States of America **101:**15196-15200.

33. **Johnson, R. F., J. Dyall, D. R. Ragland, L. Huzella, R. Byrum, C. Jett, M. St Claire, A. L. Smith, J. Paragas, J. E. Blaney, and P. B. Jahrling.** 2011. Comparative analysis of monkeypox virus infection of cynomolgus macaques by the intravenous or intrabronchial inoculation route. Journal of virology **85:**2112-2125.

34. **Johnston, S. C., K. L. Lin, J. H. Connor, G. Ruthel, A. Goff, and L. E. Hensley.** 2012. In vitro inhibition of monkeypox virus production and spread by Interferon-beta. Virology journal **9:**5.

35. **Jordan, R., and D. Hruby.** 2006. Smallpox antiviral drug development: satisfying the animal efficacy rule. Expert review of anti-infective therapy **4:**277-289.

36. **Khan, A. S., G. L. Smith, I. K. Damon, J. W. Huggins, P. B. Jahrling, B. Moss, and G. McFadden.** 2010. Scientific review of variola virus research, 1999–2010. WHO Document Production Services, WHO Document Production Services.

37. **Kulesh, D. A., B. M. Loveless, D. Norwood, J. Garrison, C. A. Whitehouse, C. Hartmann, E. Mucker, D. Miller, L. P. Wasieloski, Jr., J. Huggins, G. Huhn, L. L. Miser, C. Imig, M. Martinez, T. Larsen, C. A. Rossi, and G. V. Ludwig.** 2004. Monkeypox virus detection in rodents using real-time 3'-minor groove binder TaqMan assays on the Roche LightCycler. Laboratory investigation; a journal of technical methods and pathology **84:**1200-1208.

38. **Levine, R. S., A. T. Peterson, K. L. Yorita, D. Carroll, I. K. Damon, and M. G. Reynolds.** 2007. Ecological niche and geographic distribution of human monkeypox in Africa. PloS one **2:**e176.

39. **Likos, A. M., S. A. Sammons, V. A. Olson, A. M. Frace, Y. Li, M. Olsen-Rasmussen, W. Davidson, R. Galloway, M. L. Khristova, M. G. Reynolds, H. Zhao, D. S. Carroll, A. Curns, P. Formenty, J. J. Esposito, R. L. Regnery, and I. K. Damon.** 2005. A tale of two clades: monkeypox viruses. The Journal of general virology **86:**2661-2672.

40. **McFadden, G.** 2005. Poxvirus tropism. Nature reviews. Microbiology **3:**201-213.

41. **Moss, B.** 2012. Poxvirus cell entry: how many proteins does it take? Viruses **4:**688-707.

42. **Moss, B.** 2011. Smallpox vaccines: targets of protective immunity. Immunological reviews **239:**8-26.

43.   **Nalca, A., V. A. Livingston, N. L. Garza, E. E. Zumbrun, O. M. Frick, J. L. Chapman, and J. M. Hartings.** 2010. Experimental infection of cynomolgus macaques (Macaca fascicularis) with aerosolized monkeypox virus. PloS one **5**.

44.   **NSAR** 2005, posting date. Select agent and toxins. [Online.]

45.   **Paran, N., and G. Sutter.** 2009. Smallpox vaccines: New formulations and revised strategies for vaccination. Human vaccines **5:**824-831.

46.   **Parker, S., L. Handley, and R. M. Buller.** 2008. Therapeutic and prophylactic drugs to treat orthopoxvirus infections. Future virology **3:**595-612.

47.   **Pepin, M., M. Bouloy, B. H. Bird, A. Kemp, and J. Paweska.** 2010. Rift Valley fever virus(Bunyaviridae: Phlebovirus): an update on pathogenesis, molecular epidemiology, vectors, diagnostics and prevention. Veterinary research **41:**61.

48.   **Perdiguero, B., and M. Esteban.** 2009. The interferon system and vaccinia virus evasion mechanisms. Journal of interferon & cytokine research : the official journal of the International Society for Interferon and Cytokine Research **29:**581-598.

49.   **Prichard, M. N., and E. R. Kern.** 2012. Orthopoxvirus targets for the development of new antiviral agents. Antiviral research **94:**111-125.

50.   **Randall, R. E., and S. Goodbourn.** 2008. Interferons and viruses: an interplay between induction, signalling, antiviral responses and virus countermeasures. The Journal of general virology **89:**1-47.

51.   **Rimoin, A. W., P. M. Mulembakani, S. C. Johnston, J. O. Lloyd Smith, N. K. Kisalu, T. L. Kinkela, S. Blumberg, H. A. Thomassen, B. L. Pike, J. N. Fair, N. D. Wolfe, R. L. Shongo, B. S. Graham, P. Formenty, E. Okitolonda, L. E. Hensley, H. Meyer, L. L. Wright, and J. J. Muyembe.** 2010. Major increase in human monkeypox incidence

30 years after smallpox vaccination campaigns cease in the Democratic Republic of Congo. Proceedings of the National Academy of Sciences of the United States of America **107:**16262-16267.

52.   **Roberts, K. L., and G. L. Smith.** 2008. Vaccinia virus morphogenesis and dissemination. Trends Microbiol **16:**472-479.

53.   **Ross, T. M., N. Bhardwaj, S. J. Bissel, A. L. Hartman, and D. R. Smith.** 2012. Animal models of Rift Valley fever virus infection. Virus research **163:**417-423.

54.   **Sanchez-Puig, J. M., L. Sanchez, G. Roy, and R. Blasco.** 2004. Susceptibility of different leukocyte cell types to Vaccinia virus infection. Virology journal **1:**10.

55.   **Shaner, N. C., R. E. Campbell, P. A. Steinbach, B. N. Giepmans, A. E. Palmer, and R. Y. Tsien.** 2004. Improved monomeric red, orange and yellow fluorescent proteins derived from Discosoma sp. red fluorescent protein. Nature biotechnology **22:**1567-1572.

56.   **Stertz, S., M. Reichelt, J. Krijnse-Locker, J. Mackenzie, J. C. Simpson, O. Haller, and G. Kochs.** 2006. Interferon-induced, antiviral human MxA protein localizes to a distinct subcompartment of the smooth endoplasmic reticulum. Journal of interferon & cytokine research : the official journal of the International Society for Interferon and Cytokine Research **26:**650-660.

57.   **Stittelaar, K. J., G. van Amerongen, I. Kondova, T. Kuiken, R. F. van Lavieren, F. H. Pistoor, H. G. Niesters, G. van Doornum, B. A. van der Zeijst, L. Mateo, P. J. Chaplin, and A. D. Osterhaus.** 2005. Modified vaccinia virus Ankara protects macaques against respiratory challenge with monkeypox virus. Journal of virology **79:**7845-7851.

58.   **Traktman, P.** 1990. The enzymology of poxvirus DNA replication. Current topics in microbiology and immunology **163:**93-123.

59.	**Tsien, R. Y.** 1998. The green fluorescent protein. Annual review of biochemistry **67:**509-544.

60.	**von Krempelhuber, A., J. Vollmar, R. Pokorny, P. Rapp, N. Wulff, B. Petzold, A. Handley, L. Mateo, H. Siersbol, H. Kollaritsch, and P. Chaplin.** 2010. A randomized, double-blind, dose-finding Phase II study to evaluate immunogenicity and safety of the third generation smallpox vaccine candidate IMVAMUNE. Vaccine **28:**1209-1216.

61.	**Ward, B. M., and B. Moss.** 2001. Vaccinia virus intracellular movement is associated with microtubules and independent of actin tails. Journal of virology **75:**11651-11663.

62.	**Weimar, W., L. Stitz, A. Billiau, K. Cantell, and H. Schellekens.** 1980. Prevention of vaccinia lesions in Rhesus monkeys by human leucocyte and fibroblast interferon. The Journal of general virology **48:**25-30.

63.	**Werner, G. T., E. Metzger, and O. Sauer.** 1979. Adenine arabinoside monophosphate in experimental vaccinia virus infections. Advances in ophthalmology = Fortschritte der Augenheilkunde = Progres en ophtalmologie **38:**72-81.

64.	**Wertheim, H. F. L., P. Horby, and J. P. Woodall.** 2012. Atlas of human infectious diseases. Wiley-Blackwell, Chichester, West Sussex.

65.	**Wilck, M. B., M. S. Seaman, L. R. Baden, S. R. Walsh, L. E. Grandpre, C. Devoy, A. Giri, J. A. Kleinjan, L. C. Noble, K. E. Stevenson, H. T. Kim, and R. Dolin.** 2010. Safety and immunogenicity of modified vaccinia Ankara (ACAM3000): effect of dose and route of administration. The Journal of infectious diseases **201:**1361-1370.

66.	**Yang, G., D. C. Pevear, M. H. Davies, M. S. Collett, T. Bailey, S. Rippen, L. Barone, C. Burns, G. Rhodes, S. Tohan, J. W. Huggins, R. O. Baker, R. L. Buller, E. Touchette, K. Waller, J. Schriewer, J. Neyts, E. DeClercq, K. Jones, D. Hruby, and**

R. Jordan. 2005. An orally bioavailable antipoxvirus compound (ST-246) inhibits extracellular virus formation and protects mice from lethal orthopoxvirus Challenge. J Virol **79:**13139-13149.

67.   **Quinnan, G. V.** 1985. Vaccinia viruses as vectors for vaccine antigens : proceedings of the Workshop on Vaccinia Viruses as Vectors for Vaccine Antigens, held November 13-14, 1984, in Chevy Chase, Maryland, U.S.A. Elsevier, New York.

Clearance Letters

Virology Journal Clearance Statement
Under Open Access Agreement
For Figures 5, 7, 8, 9, 10

Confirmation of the open access agreement and unrestricted reproduction/inclusion of previously published material (data and figures) into the final written thesis was obtained through verbal communication with BioMed Central Ltd. – the publishing company for Virology Journal. No formal written permissions were required for clearance "under the terms of the Creative Commons Attribution License (http://creativecommons.org/licenses/by/2.0), which permits unrestricted use, distribution, and reproduction in any medium, provided the original work is properly cited." Permission to include data and figures for use in this thesis was cleared by Dr. Sara Johnston (primary and corresponding author) in the attached signed letter.

The full license agreement and journal contact information is provided below:

Virology Journal
c/o BioMed Central
236 Gray's Inn Road
London WC1X 8HB
United Kingdom
virologyjournal@biomedcentral.com
info@biomedcentral.com
Phone: +44 (0) 20 3192 2009

Clearance Statement
Dr. Sara C. Johnston

As primary and corresponding author, I hereby grant permission for Kenny Lin to include material from the publication "*In vitro* inhibition of monkeypox virus production and spread by Interferon-β" *Virology Journal* 2012 in his Master of Science thesis. I have reviewed the material and acknowledge the scientific contributions he provided towards this manuscript as described in the thesis.

Sara C. Johnston, Ph.D.

BioMed Central copyright and license agreement

In submitting a research article ('article') to any of the journals published by BioMed Central Ltd ('BioMed Central') I certify that:

1. I am authorized by my co-authors to enter into these arrangements.

2. I warrant, on behalf of myself and my co-authors, that:

   a. the article is original, has not been formally published in any other peer-reviewed journal, is not under consideration by any other journal and does not infringe any existing copyright or any other third party rights;

   b. I am/we are the sole author(s) of the article and have full authority to enter into this agreement and in granting rights to BioMed Central are not in breach of any other obligation. If the law requires that the article be published in the public domain, I/we will notify BioMed Central at the time of submission upon which clauses 3 through 6 inclusive do not apply;

   c. the article contains nothing that is unlawful, libellous, or which would, if published, constitute a breach of contract or of confidence or of commitment given to secrecy;

   d. I/we have taken due care to ensure the integrity of the article. To my/our - and currently accepted scientific - knowledge all statements contained in it purporting to be facts are true and any formula or instruction contained in the article will not, if followed accurately, cause any injury, illness or damage to the user.

And I agree to the following license agreement:

BioMed Central Open Access license agreement

Brief summary of the agreement

Anyone is free:

- to copy, distribute, and display the work;
- to make derivative works;
- to make commercial use of the work;

Under the following conditions: Attribution

- the original author must be given credit;
- for any reuse or distribution, it must be made clear to others what the license terms of this work are;
- any of these conditions can be waived if the authors gives permission.

Statutory fair use and other rights are in no way affected by the above.

Full BioMed Central Open Access license agreement

(Identical to the 'Creative Commons Attribution License')

License

1. Definitions

a. **"Collective Work"** means a work, such as a periodical issue, anthology or encyclopedia, in which the Work in its entirety in unmodified form, along with a number of other contributions, constituting separate and independent works in themselves, are assembled into a collective whole. A work that constitutes a Collective Work will not be considered a Derivative Work (as defined below) for the purposes of this License.

b. **"Derivative Work"** means a work based upon the Work or upon the Work and other pre-existing works, such as a translation, musical arrangement, dramatization, fictionalization, motion picture version, sound recording, art reproduction, abridgment, condensation, or any other form in which the Work may be recast, transformed, or adapted, except that a work that constitutes a Collective Work will not be considered a Derivative Work for the purpose of this License. For the avoidance of doubt, where the Work is a musical composition or sound recording, the synchronization of the Work in timed-relation with a moving image ("synching") will be considered a Derivative Work for the purpose of this License.

c. **"Licensor"** means the individual or entity that offers the Work under the terms of this License.

d. **"Original Author"** means the individual or entity who created the Work.

e. **"Work"** means the copyrightable work of authorship offered under the terms of this License.

f. **"You"** means an individual or entity exercising rights under this License who has not previously violated the terms of this License with respect to the Work, or who has received express permission from the Licensor to exercise rights under this License despite a previous violation.

2. Fair Use Rights

Nothing in this license is intended to reduce, limit, or restrict any rights arising from fair use, first sale or other limitations on the exclusive rights of the copyright owner under copyright law or other applicable laws.

3. License Grant

Subject to the terms and conditions of this License, Licensor hereby grants You a worldwide, royalty-free, non-exclusive, perpetual (for the duration of the applicable copyright) license to exercise the rights in the Work as stated below:

a. to reproduce the Work, to incorporate the Work into one or more Collective Works, and to reproduce the Work as incorporated in the Collective Works;

b. to create and reproduce Derivative Works;

c. to distribute copies or phonorecords of, display publicly, perform publicly, and perform publicly by means of a digital audio transmission the Work including as incorporated in Collective Works;

d. to distribute copies or phonorecords of, display publicly, perform publicly, and perform publicly by means of a digital audio transmission Derivative Works;

e. For the avoidance of doubt, where the work is a musical composition:

i. **Performance Royalties Under Blanket Licenses.** Licensor waives the exclusive right to collect, whether individually or via a performance rights society (e.g. ASCAP, BMI, SESAC), royalties for the public performance or public digital performance (e.g. webcast) of the Work.

ii. **Mechanical Rights and Statutory Royalties.** Licensor waives the exclusive right to collect, whether individually or via a music rights agency or designated agent (e.g. Harry Fox Agency), royalties for any phonorecord You create from the Work ("cover version") and distribute, subject to the compulsory license created by 17 USC Section 115 of the US Copyright Act (or the equivalent in other jurisdictions).

f. **Webcasting Rights and Statutory Royalties.** For the avoidance of doubt, where the Work is a sound recording, Licensor waives the exclusive right to collect, whether individually or via a performance-rights society (e.g. SoundExchange), royalties for the public digital performance (e.g. webcast) of the Work, subject to the compulsory license created by 17 USC Section 114 of the US Copyright Act (or the equivalent in other jurisdictions).

The above rights may be exercised in all media and formats whether now known or hereafter devised. The above rights include the right to make such modifications as are technically necessary to exercise the rights in other media and formats. All rights not expressly granted by Licensor are hereby reserved.

4. Restrictions

The license granted in Section 3 above is expressly made subject to and limited by the following restrictions:

a. You may distribute, publicly display, publicly perform, or publicly digitally perform the Work only under the terms of this License, and You must include a copy of, or the Uniform Resource Identifier for, this License with every copy or phonorecord of the Work You distribute, publicly display, publicly perform, or publicly digitally perform. You may not offer or impose any terms on the Work that alter or restrict the terms of this License or the recipients' exercise of the rights granted hereunder. You may not sublicense the Work. You must keep intact all notices that refer to this License and to the disclaimer of warranties. You may not distribute, publicly display, publicly perform, or publicly digitally perform the Work with any technological measures that control access or use of the Work in a manner inconsistent with the terms of this License Agreement. The above applies to the Work as incorporated in a Collective Work, but this does not require the Collective Work apart from the Work itself to be made subject to the terms of this License. If You create a Collective Work, upon notice from any Licensor You must, to the extent practicable, remove from the Collective Work any reference to such Licensor or the Original Author, as requested. If You create a Derivative Work, upon notice from any Licensor You must, to the extent practicable, remove from the Derivative Work any reference to such Licensor or the Original Author, as requested.

b. If you distribute, publicly display, publicly perform, or publicly digitally perform the Work or any Derivative Works or Collective Works, You must keep intact all copyright notices for the Work and give the Original Author credit reasonable to the medium or means You are utilizing by conveying the name (or pseudonym if applicable) of the Original Author if supplied; the title of the Work if supplied; to the extent reasonably practicable, the Uniform Resource Identifier, if any, that Licensor specifies to be associated with the Work, unless such URI does not refer to the copyright notice or licensing information for the Work; and in the case of a Derivative Work, a credit

identifying the use of the Work in the Derivative Work (e.g., "French translation of the Work by Original Author," or "Screenplay based on original Work by Original Author"). Such credit may be implemented in any reasonable manner; provided, however, that in the case of a Derivative Work or Collective Work, at a minimum such credit will appear where any other comparable authorship credit appears and in a manner at least as prominent as such other comparable authorship credit.

5. Representations, Warranties and Disclaimer
UNLESS OTHERWISE MUTUALLY AGREED TO BY THE PARTIES IN WRITING, LICENSOR OFFERS THE WORK AS-IS AND MAKES NO REPRESENTATIONS OR WARRANTIES OF ANY KIND CONCERNING THE WORK, EXPRESS, IMPLIED, STATUTORY OR OTHERWISE, INCLUDING, WITHOUT LIMITATION, WARRANTIES OF TITLE, MERCHANTIBILITY, FITNESS FOR A PARTICULAR PURPOSE, NONINFRINGEMENT, OR THE ABSENCE OF LATENT OR OTHER DEFECTS, ACCURACY, OR THE PRESENCE OF ABSENCE OF ERRORS, WHETHER OR NOT DISCOVERABLE. SOME JURISDICTIONS DO NOT ALLOW THE EXCLUSION OF IMPLIED WARRANTIES, SO SUCH EXCLUSION MAY NOT APPLY TO YOU.

6. Limitation on Liability
EXCEPT TO THE EXTENT REQUIRED BY APPLICABLE LAW, IN NO EVENT WILL LICENSOR BE LIABLE TO YOU ON ANY LEGAL THEORY FOR ANY SPECIAL, INCIDENTAL, CONSEQUENTIAL, PUNITIVE OR EXEMPLARY DAMAGES ARISING OUT OF THIS LICENSE OR THE USE OF THE WORK, EVEN IF LICENSOR HAS BEEN ADVISED OF THE POSSIBILITY OF SUCH DAMAGES.

7. Termination

a. This License and the rights granted hereunder will terminate automatically upon any breach by You of the terms of this License. Individuals or entities who have received Derivative Works or Collective Works from You under this License, however, will not have their licenses terminated provided such individuals or entities remain in full compliance with those licenses. Sections 1, 2, 5, 6, 7, and 8 will survive any termination of this License.

b. Subject to the above terms and conditions, the license granted here is perpetual (for the duration of the applicable copyright in the Work). Notwithstanding the above, Licensor reserves the right to release the Work under different license terms or to stop distributing the Work at any time; provided, however that any such election will not serve to withdraw this License (or any other license that has been, or is required to be, granted under the terms of this License), and this License will continue in full force and effect unless terminated as stated above.
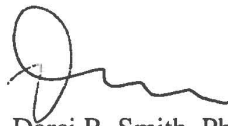
8. Miscellaneous

a. Each time You distribute or publicly digitally perform the Work or a Collective Work, the Licensor offers to the recipient a license to the Work on the same terms and conditions as the license granted to You under this License.

b. Each time You distribute or publicly digitally perform a Derivative Work, Licensor offers to the recipient a license to the original Work on the same terms and conditions as the license granted to You under this License.

c. If any provision of this License is invalid or unenforceable under applicable law, it shall not affect the validity or enforceability of the remainder of the terms of this License, and without further action by the parties to this agreement, such provision shall be reformed to the minimum extent necessary to make such provision valid and enforceable.

d. No term or provision of this License shall be deemed waived and no breach consented to unless such waiver or consent shall be in writing and signed by the party to be charged with such waiver or consent.

e. This License constitutes the entire agreement between the parties with respect to the Work licensed here. There are no understandings, agreements or representations with respect to the Work not specified here. Licensor shall not be bound by any additional provisions that may appear in any communication from You. This License may not be modified without the mutual written agreement of the Licensor and You.

Appendix A Clearance

Clearance Statement
Dr. Darci R. Smith

As principal investigator and corresponding author, I hereby grant permission for Kenny Lin to include the summary write up of material contained in the two in preparation manuscripts: "Aerosolized Rift Valley Fever Virus Exposure Causes a Significant Difference in the Chemotactic and Inflammatory Gene Expression Response in the Murine Model" and "Aerosolized Rift Valley Fever Virus Causes Earlier and More Severe Neuropathology in the Murine Model, which has Important Implications for Therapeutic Development" in his Master of Science thesis. I have reviewed the material and acknowledge the scientific contributions he provided towards these manuscripts as described in the thesis.

Darci R. Smith, Ph.D.

Figure 1: Orthopoxvirus Replication Cycle

**OXFORD UNIVERSITY PRESS LICENSE
TERMS AND CONDITIONS**

Sep 28, 2012

This is a License Agreement between Kenny Lin ("You") and Oxford University Press ("Oxford University Press") provided by Copyright Clearance Center ("CCC"). The license consists of your order details, the terms and conditions provided by Oxford University Press, and the payment terms and conditions.

All payments must be made in full to CCC. For payment instructions, please see information listed at the bottom of this form.

License Number	2997721160427
License date	Sep 28, 2012
Licensed content publisher	Oxford University Press
Licensed content publication	Nucleic Acids Research
Licensed content title	ExPASy: SIB bioinformatics resource portal:
Licensed content author	Panu Artimo, Manohar Jonnalagedda, Konstantin Arnold, Delphine Baratin, Gabor Csardi, Edouard de Castro, Séverine Duvaud, Volker Flegel, Arnaud Fortier, Elisabeth Gasteiger, Aurélien Grosdidier, Céline Hernandez, Vassilios Ioannidis, Dmitry Kuznetsov, Robin Liechti, Sébastien Moretti, Khaled Mostaguir, Nicole Redaschi, Grégoire Rossier, Ioannis Xenarios, Heinz Stockinger
Licensed content date	07/01/2012
Type of Use	Thesis/Dissertation
Institution name	
Title of your work	Generation and Characterization of a Double Recombinant Monkeypox Virus for use in Animal Model Development and Therapeutic Evaluation
Publisher of your work	n/a
Expected publication date	Oct 2012
Permissions cost	0.00 USD
Value added tax	0.00 USD
Total	0.00 USD
Total	0.00 USD

Terms and Conditions

STANDARD TERMS AND CONDITIONS FOR REPRODUCTION OF MATERIAL FROM AN OXFORD UNIVERSITY PRESS JOURNAL

1. Use of the material is restricted to the type of use specified in your order details.

2. This permission covers the use of the material in the English language in the following territory: world. If you have requested additional permission to translate this material, the terms and conditions of this reuse will be set out in clause 12.

3. This permission is limited to the particular use authorized in (1) above and does not allow you to sanction its use elsewhere in any other format other than

83

specified above, nor does it apply to quotations, images, artistic works etc that have been reproduced from other sources which may be part of the material to be used.

4. No alteration, omission or addition is made to the material without our written consent. Permission must be re-cleared with Oxford University Press if/when you decide to reprint.

5. The following credit line appears wherever the material is used: author, title, journal, year, volume, issue number, pagination, by permission of Oxford University Press or the sponsoring society if the journal is a society journal. Where a journal is being published on behalf of a learned society, the details of that society must be included in the credit line.

6. For the reproduction of a full article from an Oxford University Press journal for whatever purpose, the corresponding author of the material concerned should be informed of the proposed use. Contact details for the corresponding authors of all Oxford University Press journal contact can be found alongside either the abstract or full text of the article concerned, accessible from www.oxfordjournals.org Should there be a problem clearing these rights, please contact journals.permissions@oxfordjournals.org

7. If the credit line or acknowledgement in our publication indicates that any of the figures, images or photos was reproduced, drawn or modified from an earlier source it will be necessary for you to clear this permission with the original publisher as well. If this permission has not been obtained, please note that this material cannot be included in your publication/photocopies.

8. While you may exercise the rights licensed immediately upon issuance of the license at the end of the licensing process for the transaction, provided that you have disclosed complete and accurate details of your proposed use, no license is finally effective unless and until full payment is received from you (either by Oxford University Press or by Copyright Clearance Center (CCC)) as provided in CCC's Billing and Payment terms and conditions. If full payment is not received on a timely basis, then any license preliminarily granted shall be deemed automatically revoked and shall be void as if never granted. Further, in the event that you breach any of these terms and conditions or any of CCC's Billing and Payment terms and conditions, the license is automatically revoked and shall be void as if never granted. Use of materials as described in a revoked license, as well as any use of the materials beyond the scope of an unrevoked license, may constitute copyright infringement and Oxford University Press reserves the right to take any and all action to protect its copyright in the materials.

9. This license is personal to you and may not be sublicensed, assigned or transferred by you to any other person without Oxford University Press's written permission.

10. Oxford University Press reserves all rights not specifically granted in the combination of (i) the license details provided by you and accepted in the course of this licensing transaction, (ii) these terms and conditions and (iii) CCC's Billing and Payment terms and conditions.

11. You hereby indemnify and agree to hold harmless Oxford University Press and CCC, and their respective officers, directors, employs and agents, from and against any and all claims arising out of your use of the licensed material other than as specifically authorized pursuant to this license.

12. Other Terms and Conditions:

v1.4

If you would like to pay for this license now, please remit this license along with your payment made payable to "COPYRIGHT CLEARANCE CENTER" otherwise you will be invoiced within 48 hours of the license date. Payment should be in the form of a check or money order referencing your account number and this invoice number RLNK500867022.
Once you receive your invoice for this order, you may pay your invoice by credit card. Please follow instructions provided at that time.

Make Payment To:
Copyright Clearance Center
Dept 001
P.O. Box 843006
Boston, MA 02284-3006

For suggestions or comments regarding this order, contact RightsLink Customer Support: customercare@copyright.com or +1-877-622-5543 (toll free in the US) or +1-978-646-2777.

Gratis licenses (referencing $0 in the Total field) are free. Please retain this printable license for your reference. No payment is required.

Figure 2: Human Monkeypox Distribution in Africa

Wiley-Blackwell Book Publisher Clearance For Figure:

Wertheim, H. F. L. "Atlas of human infectious diseases" 2012.

Dear Kenny Lin,

Thank you for your email request.

Permission is granted for you to use the material requested for your thesis/dissertation subject to the usual acknowledgements and on the understanding that you will reapply for permission if you wish to distribute or publish your thesis/dissertation commercially.

Permission is granted solely for use in conjunction with the thesis, and the article may not be posted online separately.

Any third party material is expressly excluded from this permission. If any material appears within the article with credit to another source, authorisation from that source must be obtained.

Kind Regards

Emma Willcox
Permissions Assistant
Wiley

PLOS One Open Access Statement For Original Content:

Levine, R. S. "Ecological niche and geographic distribution of human monkeypox in Africa." 2007.

PLOS ONE : accelerating the publication of peer-reviewed science

Open-Access License

No Permission Required

Figure 3: Human Monkeypox Distribution in the United States

**ELSEVIER LICENSE
TERMS AND CONDITIONS**

Sep 28, 2012

This is a License Agreement between Kenny Lin ("You") and Elsevier ("Elsevier") provided by Copyright Clearance Center ("CCC"). The license consists of your order details, the terms and conditions provided by Elsevier, and the payment terms and conditions.

All payments must be made in full to CCC. For payment instructions, please see information listed at the bottom of this form.

Supplier	Elsevier Limited The Boulevard,Langford Lane Kidlington,Oxford,OX5 1GB,UK
Registered Company Number	1982084
Customer name	Kenny Lin
Customer address	1425 Porter st.
	Fort Detrick, MD 21701
License number	2997711396088
License date	Sep 28, 2012
Licensed content publisher	Elsevier
Licensed content publication	The Lancet Infectious Diseases
Licensed content title	Human monkeypox
Licensed content author	Daniel B Di Giulio,Paul B Eckburg
Licensed content date	October 2004
Licensed content volume number	4
Licensed content issue number	10
Number of pages	1
Start Page	605
End Page	0
Type of Use	reuse in a thesis/dissertation
Portion	figures/tables/illustrations
Number of figures/tables/illustrations	1
Format	both print and electronic
Are you the author of this Elsevier article?	No
Will you be translating?	No
Order reference number	
Title of your thesis/dissertation	Generation and Characterization of a Double Recombinant Monkeypox Virus for use in Animal Model Development and Therapeutic Evaluation
Expected completion date	Oct 2012
Estimated size (number of pages)	80

Elsevier VAT number	GB 494 6272 12
Permissions price	0.00 USD
VAT/Local Sales Tax	0.0 USD / 0.0 GBP
Total	0.00 USD

Terms and Conditions

INTRODUCTION

1. The publisher for this copyrighted material is Elsevier. By clicking "accept" in connection with completing this licensing transaction, you agree that the following terms and conditions apply to this transaction (along with the Billing and Payment terms and conditions established by Copyright Clearance Center, Inc. ("CCC"), at the time that you opened your Rightslink account and that are available at any time at http://myaccount.copyright.com).

GENERAL TERMS

2. Elsevier hereby grants you permission to reproduce the aforementioned material subject to the terms and conditions indicated.

3. Acknowledgement: If any part of the material to be used (for example, figures) has appeared in our publication with credit or acknowledgement to another source, permission must also be sought from that source. If such permission is not obtained then that material may not be included in your publication/copies. Suitable acknowledgement to the source must be made, either as a footnote or in a reference list at the end of your publication, as follows:

"Reprinted from Publication title, Vol /edition number, Author(s), Title of article / title of chapter, Pages No., Copyright (Year), with permission from Elsevier [OR APPLICABLE SOCIETY COPYRIGHT OWNER]." Also Lancet special credit - "Reprinted from The Lancet, Vol. number, Author(s), Title of article, Pages No., Copyright (Year), with permission from Elsevier."

4. Reproduction of this material is confined to the purpose and/or media for which permission is hereby given.

5. Altering/Modifying Material: Not Permitted. However figures and illustrations may be altered/adapted minimally to serve your work. Any other abbreviations, additions, deletions and/or any other alterations shall be made only with prior written authorization of Elsevier Ltd. (Please contact Elsevier at permissions@elsevier.com)

6. If the permission fee for the requested use of our material is waived in this instance, please be advised that your future requests for Elsevier materials may attract a fee.

7. Reservation of Rights: Publisher reserves all rights not specifically granted in the combination of (i) the license details provided by you and accepted in the course of this licensing transaction, (ii) these terms and conditions and (iii) CCC's Billing and Payment terms and conditions.

8. License Contingent Upon Payment: While you may exercise the rights licensed immediately upon issuance of the license at the end of the licensing process for the transaction, provided that you have disclosed complete and accurate details of your proposed use, no license is finally effective unless and until full payment is received from you (either by publisher or by CCC) as provided in CCC's Billing and Payment terms and conditions. If full payment is not received on a timely basis,

then any license preliminarily granted shall be deemed automatically revoked and shall be void as if never granted. Further, in the event that you breach any of these terms and conditions or any of CCC's Billing and Payment terms and conditions, the license is automatically revoked and shall be void as if never granted. Use of materials as described in a revoked license, as well as any use of the materials beyond the scope of an unrevoked license, may constitute copyright infringement and publisher reserves the right to take any and all action to protect its copyright in the materials.

9. Warranties: Publisher makes no representations or warranties with respect to the licensed material.

10. Indemnity: You hereby indemnify and agree to hold harmless publisher and CCC, and their respective officers, directors, employees and agents, from and against any and all claims arising out of your use of the licensed material other than as specifically authorized pursuant to this license.

11. No Transfer of License: This license is personal to you and may not be sublicensed, assigned, or transferred by you to any other person without publisher's written permission.

12. No Amendment Except in Writing: This license may not be amended except in a writing signed by both parties (or, in the case of publisher, by CCC on publisher's behalf).

13. Objection to Contrary Terms: Publisher hereby objects to any terms contained in any purchase order, acknowledgment, check endorsement or other writing prepared by you, which terms are inconsistent with these terms and conditions or CCC's Billing and Payment terms and conditions. These terms and conditions, together with CCC's Billing and Payment terms and conditions (which are incorporated herein), comprise the entire agreement between you and publisher (and CCC) concerning this licensing transaction. In the event of any conflict between your obligations established by these terms and conditions and those established by CCC's Billing and Payment terms and conditions, these terms and conditions shall control.

14. Revocation: Elsevier or Copyright Clearance Center may deny the permissions described in this License at their sole discretion, for any reason or no reason, with a full refund payable to you. Notice of such denial will be made using the contact information provided by you. Failure to receive such notice will not alter or invalidate the denial. In no event will Elsevier or Copyright Clearance Center be responsible or liable for any costs, expenses or damage incurred by you as a result of a denial of your permission request, other than a refund of the amount(s) paid by you to Elsevier and/or Copyright Clearance Center for denied permissions.

LIMITED LICENSE

The following terms and conditions apply only to specific license types:

15. **Translation**: This permission is granted for non-exclusive world **English** rights only unless your license was granted for translation rights. If you licensed translation rights you may only translate this content into the languages you requested. A professional translator must perform all translations and reproduce the content word for word preserving the integrity of the article. If this license is to re-use 1 or 2 figures then permission is granted for non-exclusive world rights in all languages.

16. **Website**: The following terms and conditions apply to electronic reserve and author websites:
Electronic reserve: If licensed material is to be posted to website, the web site is to be password-protected and made available only to bona fide students registered on a relevant course if:
This license was made in connection with a course,
This permission is granted for 1 year only. You may obtain a license for future website posting,
All content posted to the web site must maintain the copyright information line on the bottom of each image,
A hyper-text must be included to the Homepage of the journal from which you are licensing at http://www.sciencedirect.com/science/journal/xxxxx or the Elsevier homepage for books at http://www.elsevier.com , and
Central Storage: This license does not include permission for a scanned version of the material to be stored in a central repository such as that provided by Heron/XanEdu.

17. **Author website** for journals with the following additional clauses:

All content posted to the web site must maintain the copyright information line on the bottom of each image, and the permission granted is limited to the personal version of your paper. You are not allowed to download and post the published electronic version of your article (whether PDF or HTML, proof or final version), nor may you scan the printed edition to create an electronic version. A hyper-text must be included to the Homepage of the journal from which you are licensing at http://www.sciencedirect.com/science/journal/xxxxx . As part of our normal production process, you will receive an e-mail notice when your article appears on Elsevier's online service ScienceDirect (www.sciencedirect.com). That e-mail will include the article's Digital Object Identifier (DOI). This number provides the electronic link to the published article and should be included in the posting of your personal version. We ask that you wait until you receive this e-mail and have the DOI to do any posting.

Central Storage: This license does not include permission for a scanned version of the material to be stored in a central repository such as that provided by Heron/XanEdu.

18. **Author website** for books with the following additional clauses:
Authors are permitted to place a brief summary of their work online only.
A hyper-text must be included to the Elsevier homepage at http://www.elsevier.com . All content posted to the web site must maintain the copyright information line on the bottom of each image. You are not allowed to download and post the published electronic version of your chapter, nor may you scan the printed edition to create an electronic version.

Central Storage: This license does not include permission for a scanned version of the material to be stored in a central repository such as that provided by Heron/XanEdu.

19. **Website** (regular and for author): A hyper-text must be included to the Homepage of the journal from which you are licensing at http://www.sciencedirect.com/science/journal/xxxxx. or for books to the Elsevier homepage at http://www.elsevier.com

20. **Thesis/Dissertation**: If your license is for use in a thesis/dissertation your thesis may be submitted to your institution in either print or electronic form. Should your thesis be published commercially, please reapply for permission. These

requirements include permission for the Library and Archives of Canada to supply single copies, on demand, of the complete thesis and include permission for UMI to supply single copies, on demand, of the complete thesis. Should your thesis be published commercially, please reapply for permission.

21. **Other Conditions**:

v1.6